SUPPLEMENTAL MATERIAL

SUPPLEMENTAL METHODS:

1. Computational analysis of AngII-regulated protein-protein interactions

The 6 Angiotensin II (AngII)-regulated proteins and the two AngII receptors were used to query Integrated Interactions Database (IID) (http://ophid.utoronto.ca/iid) Version 2020-05 (PMID: 30407591) to retrieve direct physical-protein interactions among them. We have further annotated interactions with kidney and lung tissue co-expression from IID, and node color with Gene Ontology biological processes. NAViGaTOR Version 3.0.13 (PMID: 19837718) was used to visualize the resulting network. Final graphs were exported in SVG format, and finalized in Adobe Illustrator version CC2020 to produce the final image with legends (**Supplemental Figure S1**).

2. Cohort constitution

Cohort for lung tissue RT-qPCR, immunostaining and Western blotting (WB) **(Figure 2A)**

Chronic lung allograft dysfunction (CLAD) lung tissue was obtained from 33 patients between May 2015 and August 2019. Of the 33 CLAD patients, 30 were consecutive patients undergoing retransplant for CLAD, 2 underwent medical assistance in dying for CLAD, and 1 was an autopsy after death from CLAD. Of these 33 patients, 15 had restrictive allograft syndrome (RAS) phenotype, and 18 had bronchiolitis obliterans syndrome (BOS) phenotype. Control lungs came from two sources: donor lungs (DL) and lobectomy samples (LB). Ten DL were obtained at the end of cold ischemic time prior to transplantation when excess tissue remained unused due to size mismatch. Nine DL were from donation after brain death (DBD). One DL was from a donation after circulatory death (DCD) where lungs were subjected to ex vivo lung perfusion prior to transplantation. LB were obtained from 10 patients undergoing lobar resection for suspected cancer: patients were included if they had normal lung function tests, were not active smokers at the time of resection, and had minimal lung disease without cancer on the final pathological specimen used for the experiment (in the cases in which the patient would have been diagnosed with lung cancer, the specimen used was without evidence of cancer infiltration).

This cohort of samples including 10 DL and 10 LB and 33 CLAD was used in its entirety for the qPCR experiments. Immunostaining experiments were performed earlier and therefore included only samples collected up to March 2019. For immunostaining, the samples from 10 CLAD patients with the most representative bronchiolitis obliterans and pleuroparenchymal fibroelastosis histology, were selected to constitute a cohort of 5 BOS and 5 RAS. Three DL and 2 LB specimens were randomly selected as controls for the immunostaining experiments. For confirmatory WB experiments, we randomly selected 4 patients

from the control group and 4 from the RAS group. These numbers were to allow loading on one gel, including one positive control and ladder. The specimens were retrieved from the same lung and adjacent location to the ones used for immunostaining and RT-qPCR experiments. The selection of samples in the two restricted cohorts (immunostaining and WB) was performed *a priori*.

Bronchoscopy and BAL protocol for BAL protein analysis cohort **(Figure 2B)**

The inclusion criteria and the clinical groups derived from our screening of all lung transplant recipients at our center from January 2019 to April 2019 are presented in the main manuscript text and in Figure 2B. LTx recipients at our center routinely undergo surveillance bronchoscopy at 0.5, 1.5, 3, 6, 9, 12, 18, and 24 months post-transplant and also when clinically indicated. The bronchoscopy procedure consists of airway inspection followed by BAL collection whereby the bronchoscope is wedged in the right middle lobe, lingula, or other lobe of interest; 50 mL of normal saline is instilled twice, each time followed by aspiration of the liquid[1].

3. Experimental analysis of lung tissue

Sample processing

All lung tissue samples were processed within 1 h of explant or resection. The time from death to processing (3 CLAD samples) was less than 3h. After dissection, samples of approximate 2 cm^2 size were submerged in 10% Formalin, transferred to 70% EtOH after 24 h, and subsequently embedded in paraffin. Separate samples for RT-qPCR were placed in RNAlater (QIAGEN) at 4°C for 24 h, decanted, and stored at -80°C. Finally, snap-frozen samples were collected for subsequent protein extraction for WB.

Histology, Immunostaining and Quantification approach

4 µm sections of formalin-fixed paraffin-embedded lung tissue were used for hematoxylin and eosin, Elastic Trichrome, and immunostaining. Slides for immunostaining were subjected to antigen retrieval (Dako antigen retrieval pH 6) in the autoclave for 15 min 121-degree steam mode), blocking with Dako protein block, and for immunohistochemistry, quenching of endogenous peroxidase activity using 3% (vol/vol) H_2O_2 for 30 min. Immunostaining was performed with purified rabbit anti-AGTR1 IgG (NBP1-77078, Novus Biologicals, Centennial, USA), rabbit anti-AGTR2 IgG (NBP1-77368, Novus Biologicals, Centennial, USA), mouse anti-TSP1 IgG1 (MA5-13398, ThermoFisher Scientific, Waltham, USA), mouse anti-GLNA IgG1 (ab64613, Abcam, Cambridge, UK), mouse anti-PanCK IgG1 [C-11] (ab7753, Abcam, Cambridge, UK), mouse anti-CD45 (BV605, BD Horizon, Franklin Lakes, USA), mouse IgG2a anti α-SMA (14-9760-82, ThermoFisher Scientific, Waltham, USA), and Rabbit anti-CD68 IgG (NBP2-48923, Novus

Biologicals, Centennial, USA). **Supplemental Figures S2, S8 and S9** show positive staining (in kidney as positive control as well as in the lung) and secondary antibody only staining for each protein of interest.

After immunofluorescence staining (AGTR1 and AGTR2), the entire slide was digitized at high resolution with the Zeiss AxioScan at a 20X power. For immunofluorescence quantification, we used Halo software (Indica Labs) for the automated quantification of positive cells (CytoNuclear FL v1.4 algorithm). The algorithm identified cells by their nucleus (DAPI) and identified AGTR1 and AGTR2 positive cells if the related fluorescence was present in a pre-defined radius from the nucleus. All parameters were kept constant for quantitative comparison between slides, using a medium-high threshold for positive staining to avoid false positives that could be related to uneven background fluorescence from slide to slide. We applied the algorithm to the entire tissue without exclusion; specifically, we did not exclude vascular structures as every lung sample was flushed, thus decreasing the risk of counting intravascular cells.

After immunohistochemistry staining (TSP1 and GLNA), the entire slide was digitized at high resolution with the Aperio CS2 scan at a 20X power. For immunohistochemistry, we used semi-quantitative scoring of the staining. Each sample was first assessed at low power magnification to evaluate the overall extent of positive staining and subsequently at high power with a focus on 8-10 zones of interest corresponding to alveolar zones, interstitial fibrosis, subpleural regions, peri-airways, and perivascular zones. Zones shown were representative of the overall staining pattern of the entire slide. Two independent reviewers (that were blinded to the group-assignment of the slides) scored independently each slide. The results of the scoring of the two reviewers were averaged to derive the final assessment score. For TSP1, as the expected immunoreactivity pattern was both intra- and extracellular, we quantified the total surface staining. For GLNA, as the staining pattern was exclusively cellular, we quantified the proportion of positively staining cells. Examples of the staining scale for TSP1 and GLNA are shown in **Supplemental Figure S12**).

The extent of parenchymal fibrosis was assessed by two independent reviewers estimating the percentage of lung parenchyma affected by pulmonary fibrosis at low power magnification. The quantification method was validated by an expert pathologist. We performed a simple linear regression between the extent of parenchymal fibrosis and the immunostaining score for each protein of interest.

RT-qPCR

Total RNA was extracted from frozen lung tissue using RNAeasy Mini Kit (QIAGEN, Mississauga, ON). Quantity and quality of RNA samples were measured using NanoDrop spectrophotometer (Thermo Scientific Canada, Nepean, ON). Each sample was analyzed in duplicate. Negative template controls were included. Oligonucleotide primer pairs are listed in **Supplemental Table 3** (final concentration of 250 nM).

Expression of each target gene was normalized to housekeeping gene Ppia (Peptidylprolyl isomerase A) and transcript levels were analyzed using the ddCt method.

A mean of 33582 ng (SD 22929 ng) of RNA was extracted per sample with median ratio 260/280 of 2.06 (IQR 2.03-2.08). cDNA was synthesized from 2 ug of total RNA using iScript advanced cDNA synthesis kit (Bio-Rad Laboratories, Mississauga, ON). The reaction mixture was incubated at 25°C, 5 min; 46°C, 20 min; 95°C, 1 min. RT-qPCR was performed on Bio-Rad CFX384 Touch™ Real-time PCR Detection System. The PCR reaction mixture contained 3 µl diluted (1:10) cDNA, 1 µl PCR primers (10 µM), 5 µl SsoAdvanced™ Universal SYBR® Green Supermix, 1 µl dH_2O. The PCR protocol was set-up for 45 cycles as 95°C, 10 sec; 60°C, 30 sec.

The melting curves of AGTR1, AGTR2, TSP1, GLNA, LYPA1 and BST1 are shown in **Supplemental Figure S6**. The separation of the amplicons on agarose gel showing only one band for each amplicon is shown in **Supplemental Figure S7**.

Protein extraction and Western blotting (**Supplemental Figure 10**)

To be able to load the samples on a 10-well gel, the WB cohort included 4 controls (2 LB and 2 DL) and 4 RAS lung tissue samples. Frozen human lung tissue samples were pulverized in liquid nitrogen to fine powders and mixed with 1 mL of extraction buffer [50 mmol/L Tris-HCl buffer (pH 8.0) containing 150 mmol/L NaCl, 5 mmol/L EDTA, 10 g/L NP-40 surfactant]. The mixtures were incubated on ice for 30 min with repeated vortex mixing every 10 min and sonicated three times for 10 sec, to break up the tissue further. Mixtures were centrifuged at 15,000 g at 4°C for 30 min, and the supernatants were used as tissue extracts. Supernatants were stored at −80 °C until use. Protein content was determined by a colorimetric assay (Bio-Rad). 10 ug of protein extracts were separated by sodium dodecyl sulfate-polyacrylamide gel electrophoresis (SDS-PAGE) using 10% or 4-15% gradient polyacrylamide gels and transferred to polyvinylidene difluoride membrane (Millipore). After incubation with 5% non-fat milk or 3% BSA in TBST (10 mM Tris, pH 8.0, 150 mM NaCl, 0.5% Tween 20) for 60 min, the membrane was incubated with mouse anti-GLNA IgG1 (1:400, ab64613, Abcam, Cambridge, UK) or mouse anti-TSP1 IgG1 (1:200, MA5-13398, ThermoFisher Scientific, Waltham, USA), respectively, at 4 °C overnight. Control for protein loading was performed by incubating membranes with a mouse monoclonal antibody for vinculin (mab6896, R&D systems) and Glyceraldehyde-3-Phosphate Dehydrogenase (GAPDH) (6C5, Millipore Sigma), respectively. In all cases the secondary antibody was horseradish peroxidase-conjugated anti-mouse (P0447, Dako). Following washing the membranes were developed with the ECL system (Amersham Biosciences)

according to manufacturer's instructions and protein bands were visualized using Image LabTM Software (Bio-Rad Laboratories). Finally, bands were quantified by densitometry using ImageJ software.

4. BAL mass-spectrometry for peptide analysis

BAL samples were thawed in a water bath at room temperature. Freeze-thaw cycles were minimized. The total protein content of each sample was measured using BCA protein colorimetric assay (Pierce). BAL volume corresponding to 100 µg from each sample was used as starting material (**Figure 1**). To assess reproducibility and recovery, 1 µg bovine serum albumin (BSA) (proteomics-grade, >98% pure, Sigma-Aldrich) was first added to each sample. Samples were then precipitated overnight with acetonitrile at a ratio of 1:9 (V/V), as previously described[2], and centrifuged at 3220 g for 30 min at 4°C. Protein pellets then underwent 3 cycles of washing with ACN, bath sonication and rigorous vortexing, followed by air-drying. Pellets were denatured in 100 µL of 8 M urea in 0.1 M of ammonium bicarbonate (Sigma-Aldrich). Samples were reduced with 20 mM dithiotreitol (Sigma-Aldrich) at 37°C for 30 min and alkylated with 80 mM iodoacetamide (Sigma-Aldrich) at RT for 30 min in the dark. Purified peptides with lysine or arginine C-terminal 13C/15N-labels and a quantitation tag (JPT Peptide technologies) were spiked into all samples at a known final concentration and the samples were incubated with Lys-C/trypsin (1:50 w/w) (Promega) at 37°C for 3 h. Protein digestion was continued by adding 0.1 M ammonium bicarbonate to reduce urea concentration to 2 M and incubating the samples at 37°C overnight. The reaction was stopped by the addition of formic acid at 1% (v/v). Samples were then vortexed, centrifuged and separated into aliquots containing 25 µg of total protein and frozen at −20°C until further analysis. After thawing, 500 fmols of three crude heavy isotope-labeled proteotypic peptides of BSA were spiked in each one to assess BSA recovery. Samples were then centrifuged at max speed for 10 min and supernatants were retained. Peptides were concentrated using C18 OMIX tips (Agilent), then eluted in 3 µL of 65% ACN solution and further diluted with 41 µL of 0.1% formic acid in water. Native peptides corresponding to AngII-regulated proteins and their matching heavy peptides are listed in **Supplemental Table S4**.

<u>Selection of proteins and peptides for parallel reaction monitoring (PRM) method development</u>

PRM methods were developed for the previously identified AngII-regulated proteins[3]. Two proteotypic peptides per AngII-regulated protein (with the exception of RHOB) were selected), using our previously acquired data from discovery experiments and Peptide Atlas Database (http://www.peptideatlas.org). The second peptide chosen for RHOB was excluded from the final PRM assays due to poor performance. Skyline software (MacCoss Lab Software, Seattle, WA) was then used for the *in-silico* digestion of the proteins. Fully tryptic peptides, 7-20 amino acids long, were chosen. Peptides with proline were preferred whereas those with methionine, tryptophan and N-terminal cysteine residues were avoided. All peptides

were searched with the protein Basic Local Alignment Tool (http://blast.ncbi.nlm.nih.gov/Blast.cgi) to ensure that the selected peptides were proteotypic to each protein.

Unscheduled survey PRM assays were designed for Q-Exactive plus™ Hybrid Quadrupole-Orbitrap™ Mass Spectrometer (Thermo Scientific), using Skyline. These assays were then used to analyze a digested pool of BAL samples containing AngII-regulated proteins, and spiked-in heavy labeled counterparts. Visual inspection of the peaks was applied to identify all precursor heavy peptides and transitions pairs. The 3-7 most intense and least noisy transitions were empirically selected to be monitored in the final method for each peptide.

A light peptide was considered present if its transitions coeluted and if the order of transitions and retention time was identical to those produced by its heavy counterpart (**Figure 1**).

Following optimization of collision energy, quadrupole isolation width and fill time **(Supplemental Figures S14 and S15, respectively)** we created methods with 5 min windows for monitoring each native peptide and its heavy-labeled counterpart. The final methods and parameters are in **Supplemental Table 4**.

Chromatographic conditions and MS analysis

PRM experiments were performed on a Q-Exactive™ Plus Hybrid Quadrupole-Orbitrap Mass Spectrometer). The tryptic peptides were loaded on a 3 cm long C18 (5 µm) trap precolumn (i.d. 200 µm) via EASY-nLC 1000 pump (Thermo Scientific) at 8 µL/min. Mobile phases included 0.1% formic acid in water (buffer A) and 0.1% formic acid in acetonitrile (buffer B). Peptides were separated with a 15 cm long C18 (3 µm) analytical column with 8 µm tip (New Objective, Woburn, MA) on a 60 min gradient elution at 300 nL/min. A five-step gradient was used: 1% to 5% of buffer B for 2 min, 5% to 35% for 47 min, 35% to 65% for 3 min, 65% to 100% for 1 min, and 100% for 7 min at 450 nL/min. One full MS1 scan was acquired in quadrupole with automatic gain control (AGC) of $1*10^6$ with a maximum injection time of 50 ms and a resolving power of 70,000 at 200 m/z. For PRM settings, MS transitions in the orbitrap were acquired with 17,500 resolving power at 200 m/z. AGC target was set to $2*10^5$ with a maximum injection time of 50 ms and isolation window of 0.6 m/z.

Assay Linearity

Assay linearity was assessed only for these peptides confidently detected in the BAL samples. Linearity was determined using a pool of BAL samples, spiked with different amounts of heavy labeled peptides. Digestion of the sample was then performed as described above for each BAL pool containing the heavy peptide in increasing final concentration, and the light/endogenous peptide in constant concentration. The intensity area ratios of heavy-labeled peptides divided by the corresponding endogenous light peptides were plotted against the spiked heavy peptide concentrations. The samples representing each

point of the linearity curve were run in duplicates and on two different days to assess repeatability and reproducibility (within-run and between-run variability) of the PRM methods and data were inspected manually. PRM assays showed excellent linearity with r^2 >0.95 for all peptides (**Supplemental Figure S16**). Mean within-run CV for each peptide was <5% except for one peptide (LVLCEVFK, GLNA protein) with CV 7%. Between-run variability demonstrated mean CVs ≤10%.

Mass-Spectrometry Data Analysis

BAL samples were randomized and run in duplicate. For quantification, the average light-to-heavy ratio was multiplied by the amount of the heavy-labeled spiked-in peptide to calculate the relative amount (fmols) of endogenous light peptide. To calculate the concentration of endogenous light peptide in each sample, this amount was divided by the volume of BAL sample used for digestion. Recovery of BSA peptides was calculated as (observed BSA)/(spiked-in BSA) × 100%. Observed BSA amount was calculated as (light-to-heavy peptide ratio) x (the amount of the heavy-labeled spiked-in BSA peptide). Distribution of peptide concentrations was assessed by Kolmogorov-Smirnov test. The differences in concentrations of peptides between groups were assessed using non-parametric tests in GraphPad Prism (version 8).

SUPPLEMENTAL ACKNOWLEDGEMENTS:

LIST OF PEOPLE WHO CONTRIBUTED TO CLAD LUNG AND CONTROL LUNG BIOBANKING

The authors would like to thank all the students, fellows, and technicians who participated in the processing of lung tissue, which was often done with short notice at difficult times of the night: Matthew White, Sajad Moshkelgosha, Betty Joe, Gafoor Puthiyaveetil, Akihiro Takahagi, Mitsuaki Kawashima, Tatsuaki Watanabe, Christina Lam, Goodness Madu, Nadia Sachewsky, Daniel Vosoughi, Madalina Maxim, Kristen Bounstra, Yohei Taniguchi, and Alexander Tigert.

REFERENCES FOR SUPPLEMENTAL MATERIAL

1. Martinu T, Koutsokera A, Benden C, Cantu E, Chambers D, Cypel M, Edelman J, Emtiazjoo A, Fisher AJ, Greenland JR, Hayes D, Jr., Hwang D, Keller BC, Lease ED, Perch M, Sato M, Todd JL, Verleden S, von der Thüsen J, Weigt SS, Keshavjee S. International Society for Heart and Lung Transplantation consensus statement for the standardization of bronchoalveolar lavage in lung transplantation. *J Heart Lung Transplant* 2020: 39(11): 1171-1190.

2. Konvalinka A, Batruch I, Tokar T, Dimitromanolakis A, Reid S, Song X, Pei Y, Drabovich AP, Diamandis EP, Jurisica I, Scholey JW. Quantification of angiotensin II-regulated proteins in urine of patients with polycystic and other chronic kidney diseases by selected reaction monitoring. *Clinical Proteomics* 2016: 13(1): 16.

3. Konvalinka A, Zhou J, Dimitromanolakis A, Drabovich AP, Fang F, Gurley S, Coffman T, John R, Zhang SL, Diamandis EP, Scholey JW. Determination of an angiotensin II-regulated proteome in primary human kidney cells by stable isotope labeling of amino acids in cell culture (SILAC). *J Biol Chem* 2013: 288(34): 24834-24847.

Supplemental Figure S1: Protein-protein interactions of AngII-regulated proteins and AngII receptors.

The six AngII-regulated proteins (Ras Homolog Family Member B (RHOB), Bone Marrow Stromal Cell Antigen 1 (BST1), Lysophospholipase 1 (LYPA1), Glutamine Synthetase (GLNA), Thrombospondin 1 (TSP1), and Laminin Subunit β2 (LAMB2)), AGTR1 and AGTR2 are depicted at the center of the interactome as big squares. All other proteins (nodes) are represented as small squares. Each line represents a direct interaction between any two proteins. Green lines indicate that these physical interactions are present in both kidney and lung. Blue and burgundy lines indicate that the interactions are known only in the lung or the kidney, respectively. Finally, those proteins previously strongly implicated in fibrosis or inflammation are circled in red. Color code annotation for proteins in the network represents gene ontology (GO) biological processes as per legend. *LYPA1, lysophospholipase 1; BST1, bone marrow Stromal cell antigen 1; GLNA, glutamine synthetase; TSP1, thrombospondin 1; LAMB2, laminin Subunit β2, RHOB, ras homolog family member B; AGTR1, angiotensin II type I receptor; AGTR2, angiotensin II type II receptor.*

S1

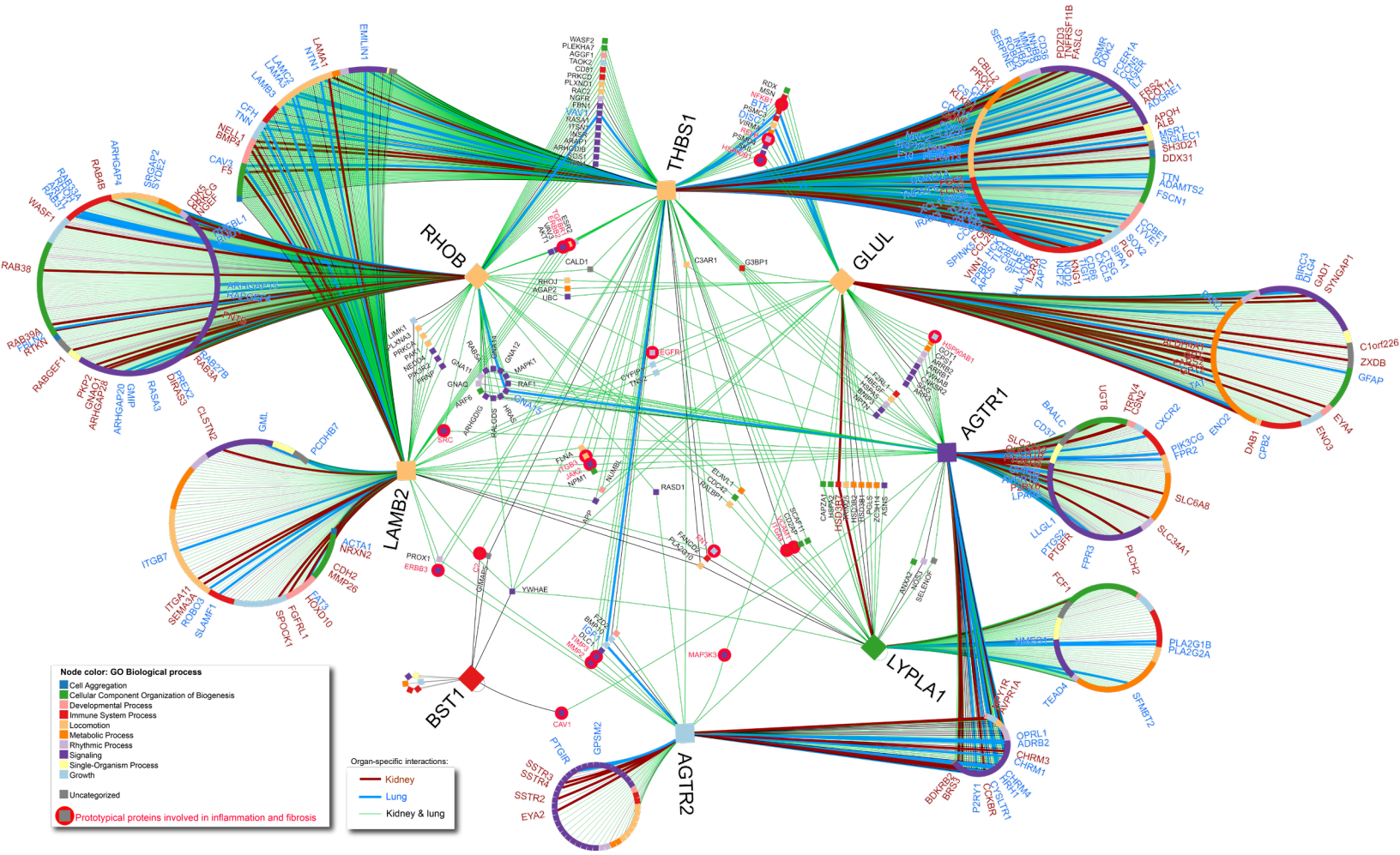
THBS1
RHOB
GLUL
AGTR1
LAMB2
LYPLA1
BST1
AGTR2
Node color: GO Biological process
Cell Aggregation
Cellular Component Organization of Biogenesis
Developmental Process
Immune System Process
Locomotion
Metabolic Process
Rhythmic Process
Signaling
Single-Organism Process
Growth
Uncategorized
Prototypical proteins involved in inflammation and fibrosis
Organ-specific interactions:
Kidney
Lung
Kidney & lung

Supplemental Figure S2: AGTR1 and AGTR2 immunostaining controls.

(A) Positive staining and secondary antibody only for AGTR1 and AGTR2 in human kidney. As expected, the positive staining is mainly localized in the tubules. (B) Positive staining and secondary antibody only of AGTR1 and AGTR2 in human CLAD lungs. *AGTR1, Angiotensin II type I receptor; AGTR2, Angiotensin II type II receptor.*

S2

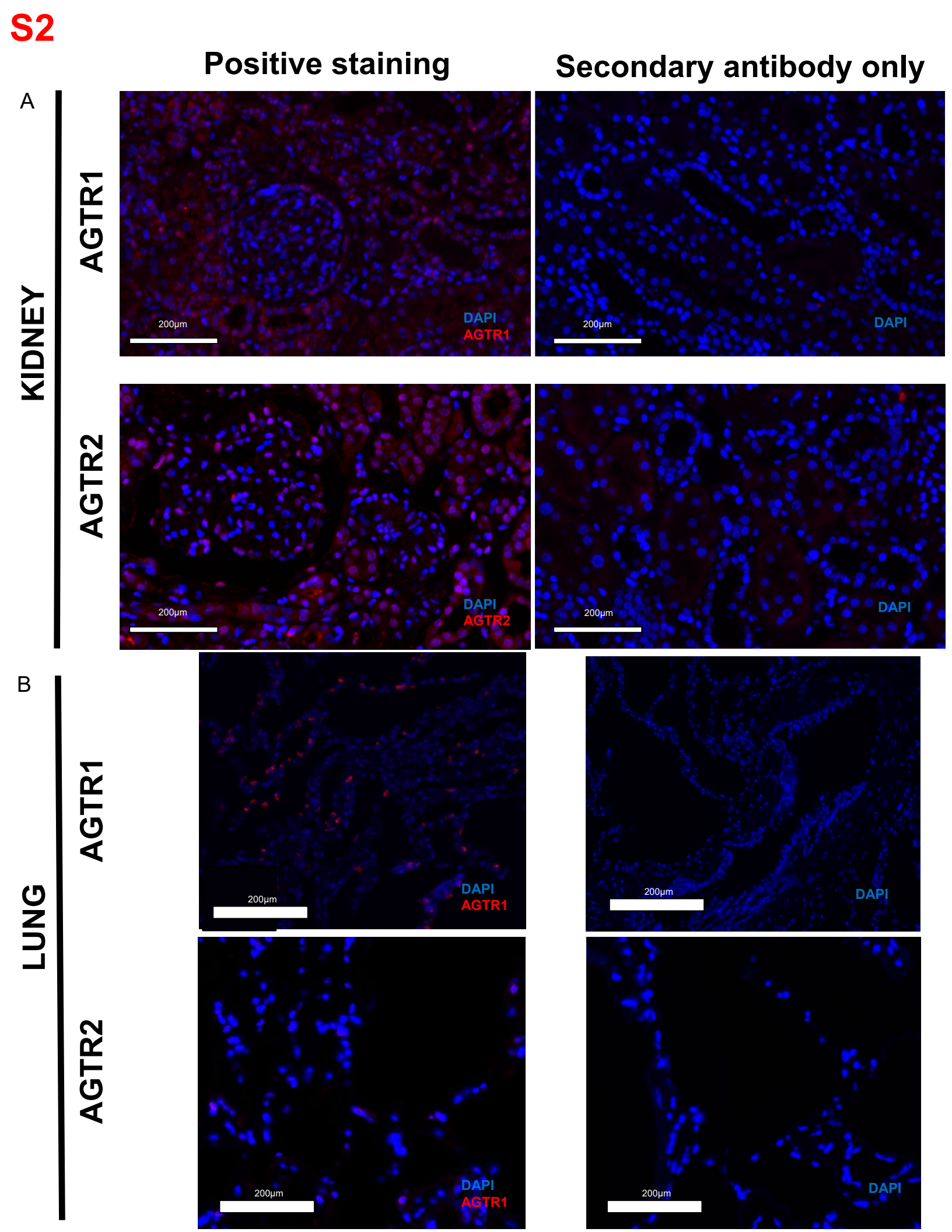
Positive staining
Secondary antibody only
A
KIDNEY
AGTR1
AGTR2
200μm
DAPI
AGTR1
AGTR2
B
LUNG

Supplemental Figure S3: Angiotensin II receptor immunoreactivity in lung tissue.

(A) Immunofluorescence quantification analyses of total number of AGTR1+ cells in 5 controls and 10 CLAD specimens, and in 5 BOS and 5 RAS. (B) % of AGTR1+ cells in 5 controls and 10 CLAD specimens, and in 5 BOS and 5 RAS. (C) Total number of AGTR2+ cells in 5 controls and 10 CLAD specimens, and in 5 BOS and 5 RAS. (D) % of AGTR2+ cells in 5 controls and 10 CLAD specimens, and in 5 BOS and 5 RAS. (E) The total cellularity of 5 control, 5 BOS and 5 RAS specimens, expressed as total number of cells per sample and per mm^2.

S3

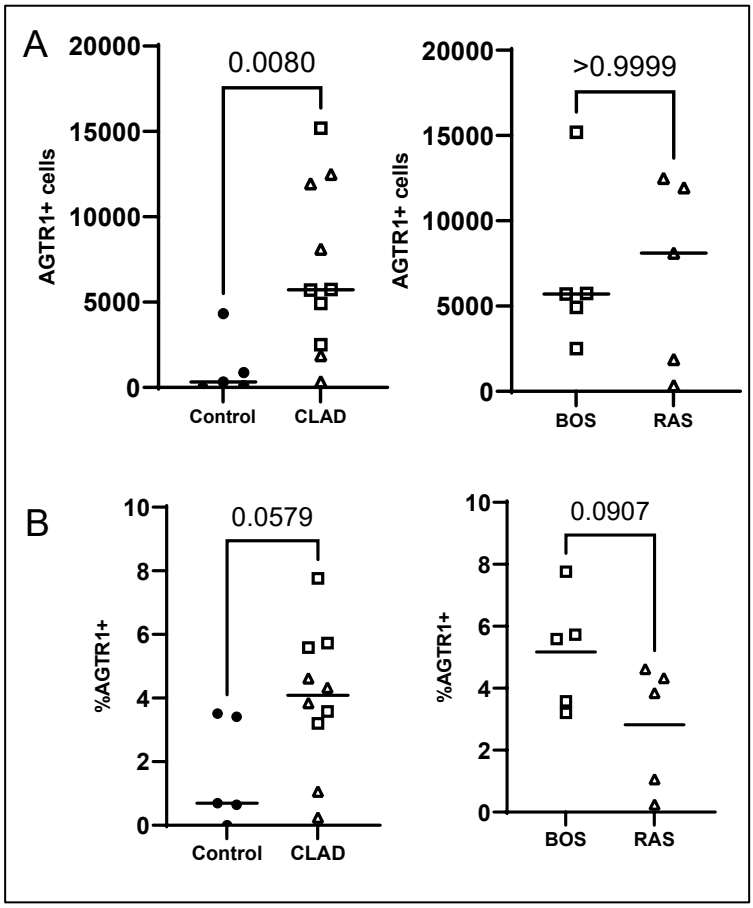
A
AGTR1+ cells
20000
15000
10000
5000
0
0.0080
Control
CLAD
>0.9999
BOS
RAS
B
%AGTR1+
10
8
6
4
2
0
0.0579
0.0907

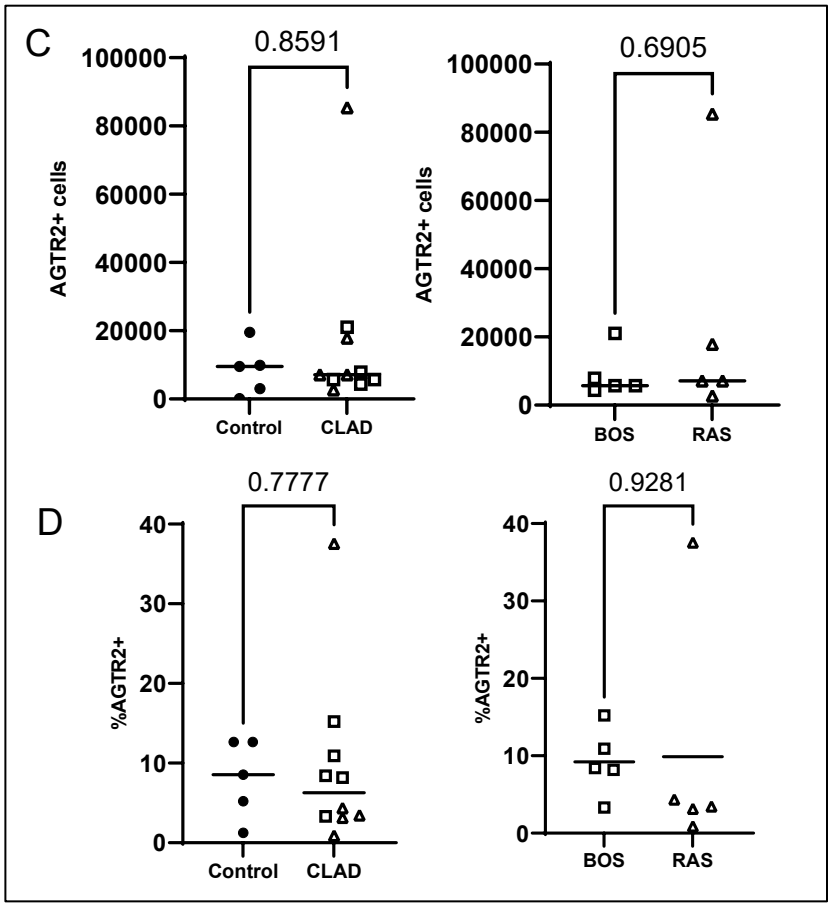
C
AGTR2+ cells
100000
80000
60000
40000
20000
0
0.8591
0.6905
Control
CLAD
BOS
RAS
D
%AGTR2+
40
30
20
10
0
0.7777
0.9281

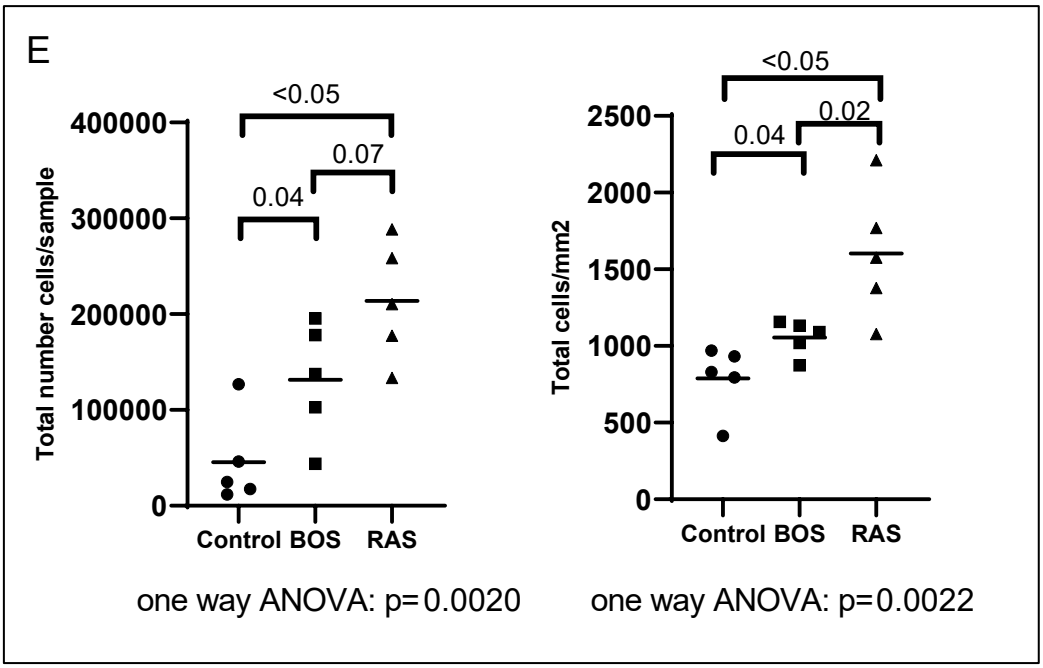
E
Total number cells/sample
400000
300000
200000
100000
0
<0.05
0.07
0.04
Control BOS RAS
one way ANOVA: p=0.0020
Total cells/mm2
2500
2000
1500
1000
500
0
<0.05
0.02
0.04
Control BOS RAS
one way ANOVA: p=0.0022

Supplemental Figure S4: Immune cells co-stain for Angiotensin II receptors in lung tissue.

(A, B and C) AGTR1 (in green) co-staining with α-smooth muscle actin (α-SMA) in red, (B) pan-cytokeratin (panCK) in turquoise, (C) and CD45 (in turquoise). (D) AGTR2 (in red) co-staining with CD45 (in green). These panels show no co-staining of AGTR1 with α-SMA or panCK, suggesting a lack of AGTR1 in myofibroblasts and pulmonary epithelial cells. On the other hand, we note positive co-staining of both AGTR1 and AGTR2 with CD45, suggesting AGTR1 and AGTR2 presence in immune cells.

S4

A

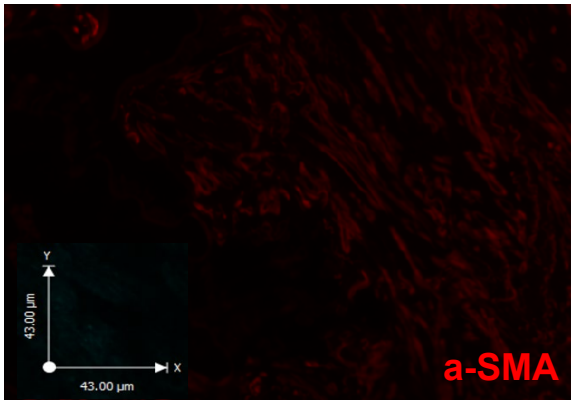
a-SMA
Y
43.00 µm
X
43.00 µm

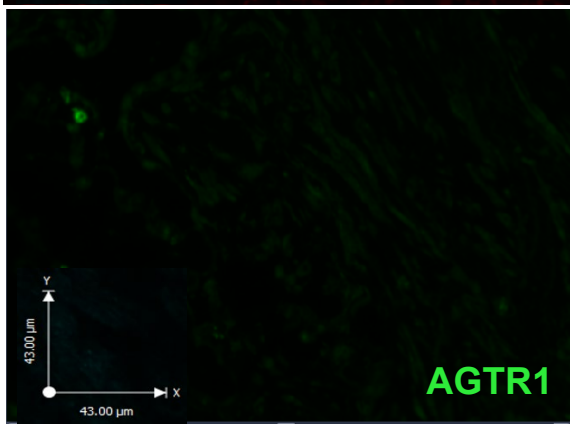
AGTR1
Y
43.00 µm
X
43.00 µm

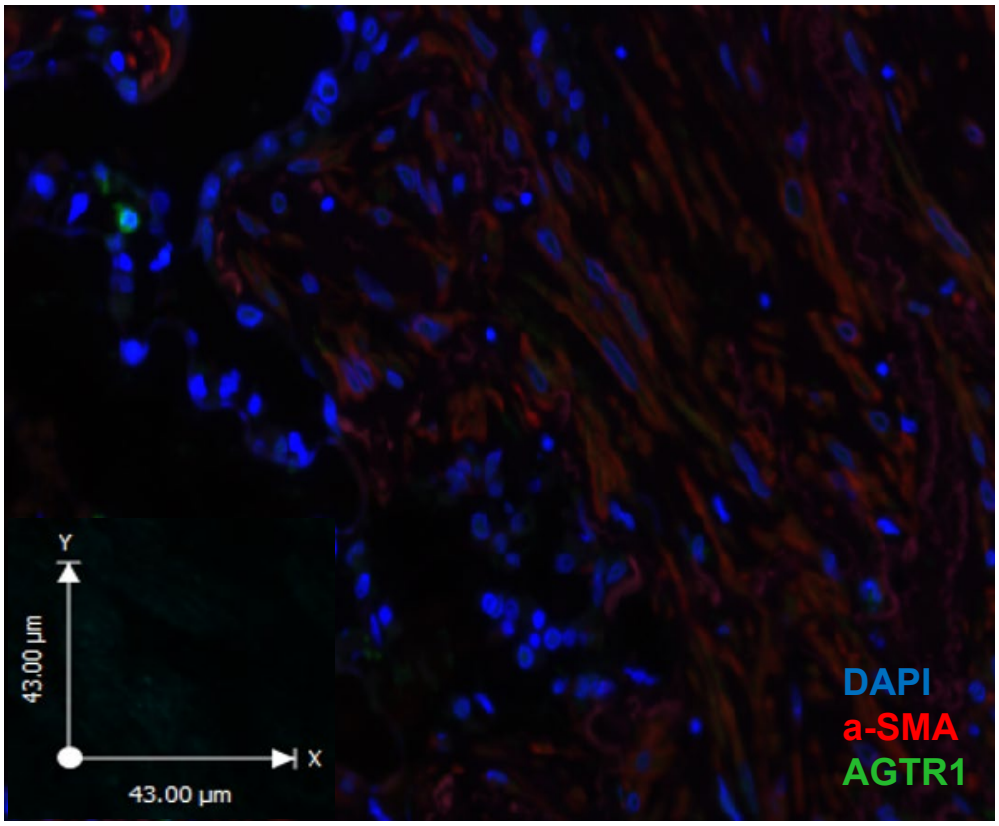
DAPI
a-SMA
AGTR1
Y
43.00 µm
X
43.00 µm

B

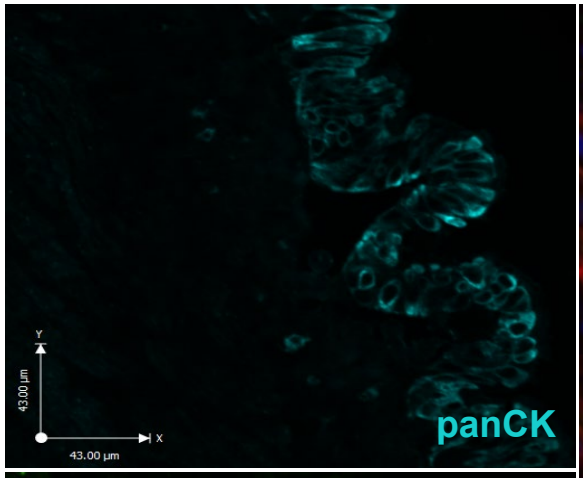
panCK
Y
43.00 µm
X
43.00 µm

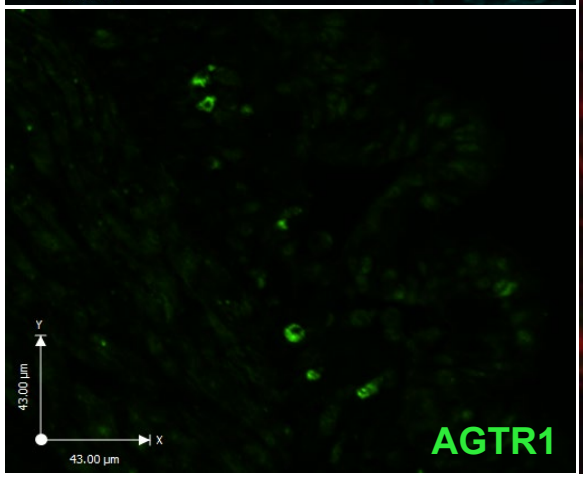
AGTR1
Y
43.00 µm
X
43.00 µm

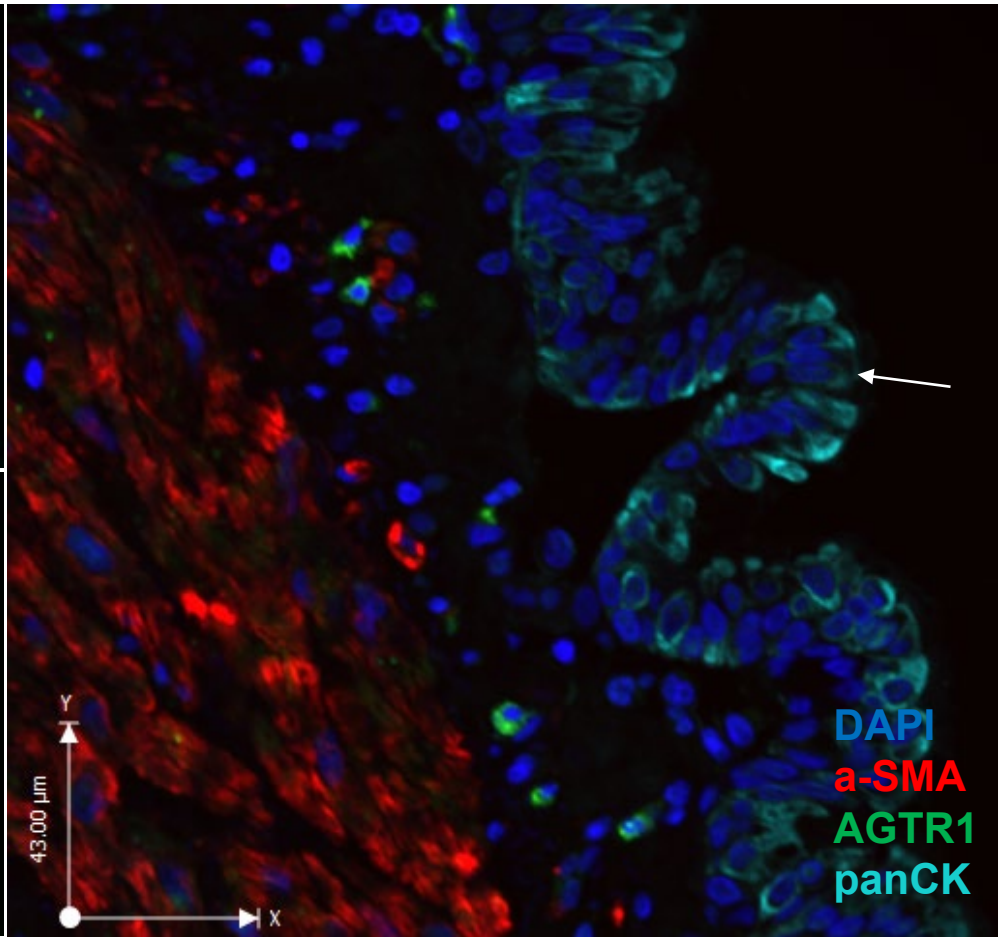
DAPI
a-SMA
AGTR1
panCK
Y
43.00 µm
X

C

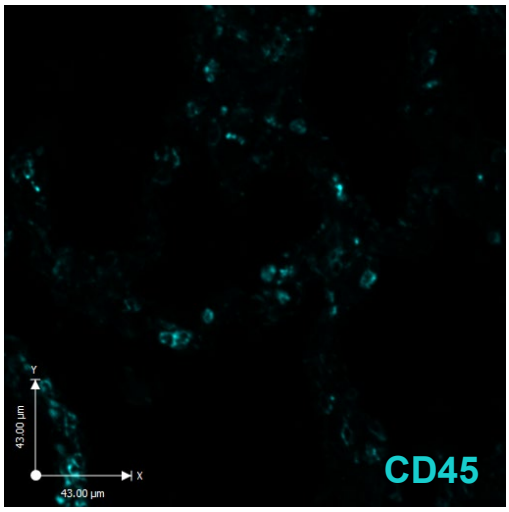
CD45
Y
43.00 µm
X
43.00 µm

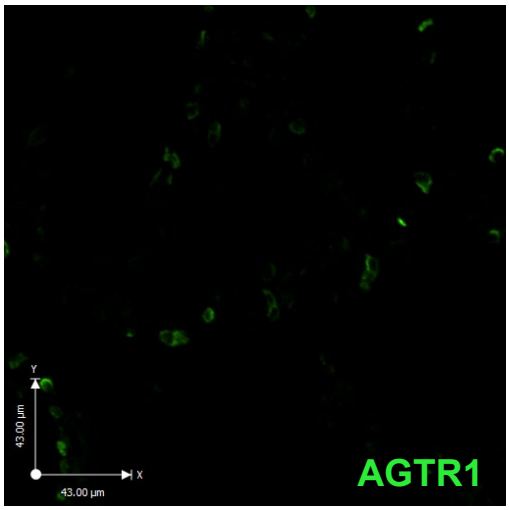
AGTR1
Y
43.00 µm
X
43.00 µm

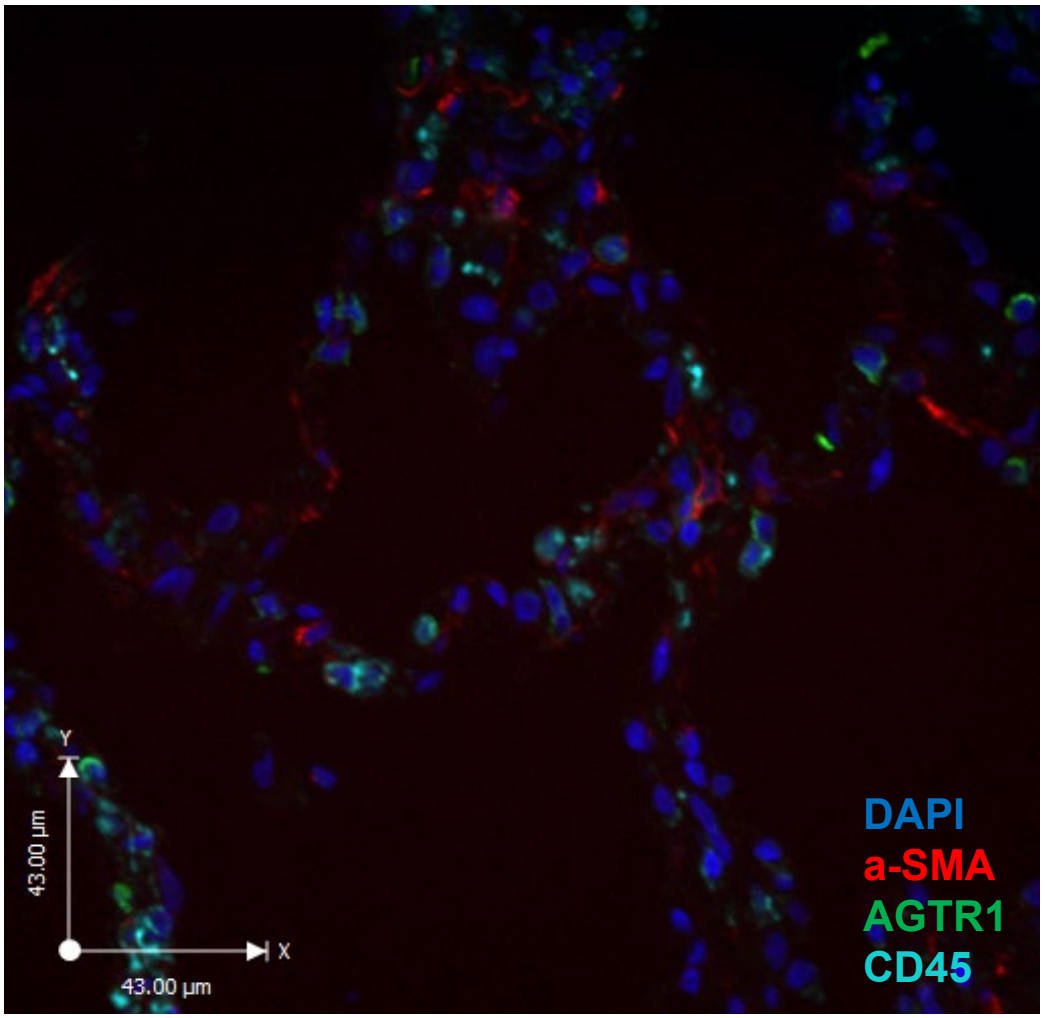
DAPI
a-SMA
AGTR1
CD45
Y
43.00 µm
X
43.00 µm

D

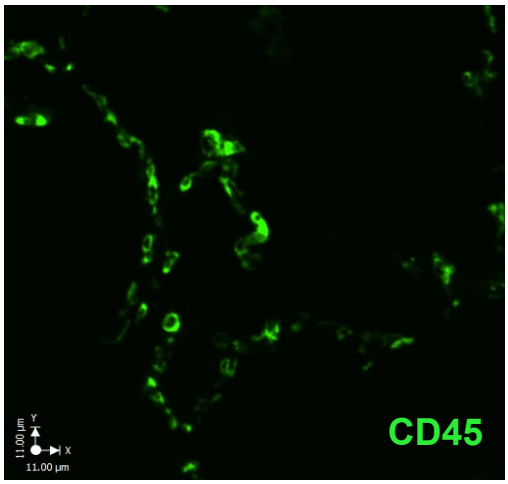
CD45
Y
11.00 µm
X
11.00 µm

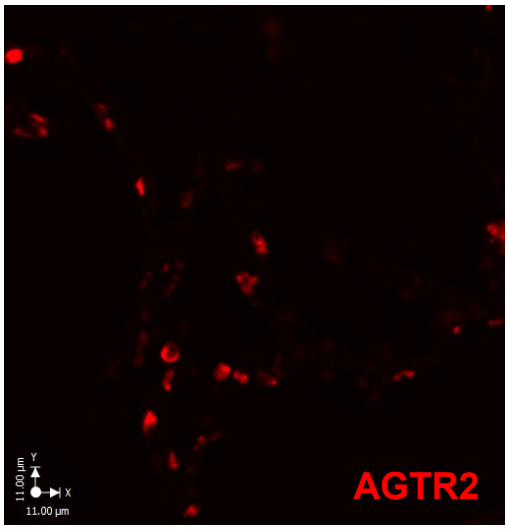
AGTR2
Y
11.00 µm
X
11.00 µm

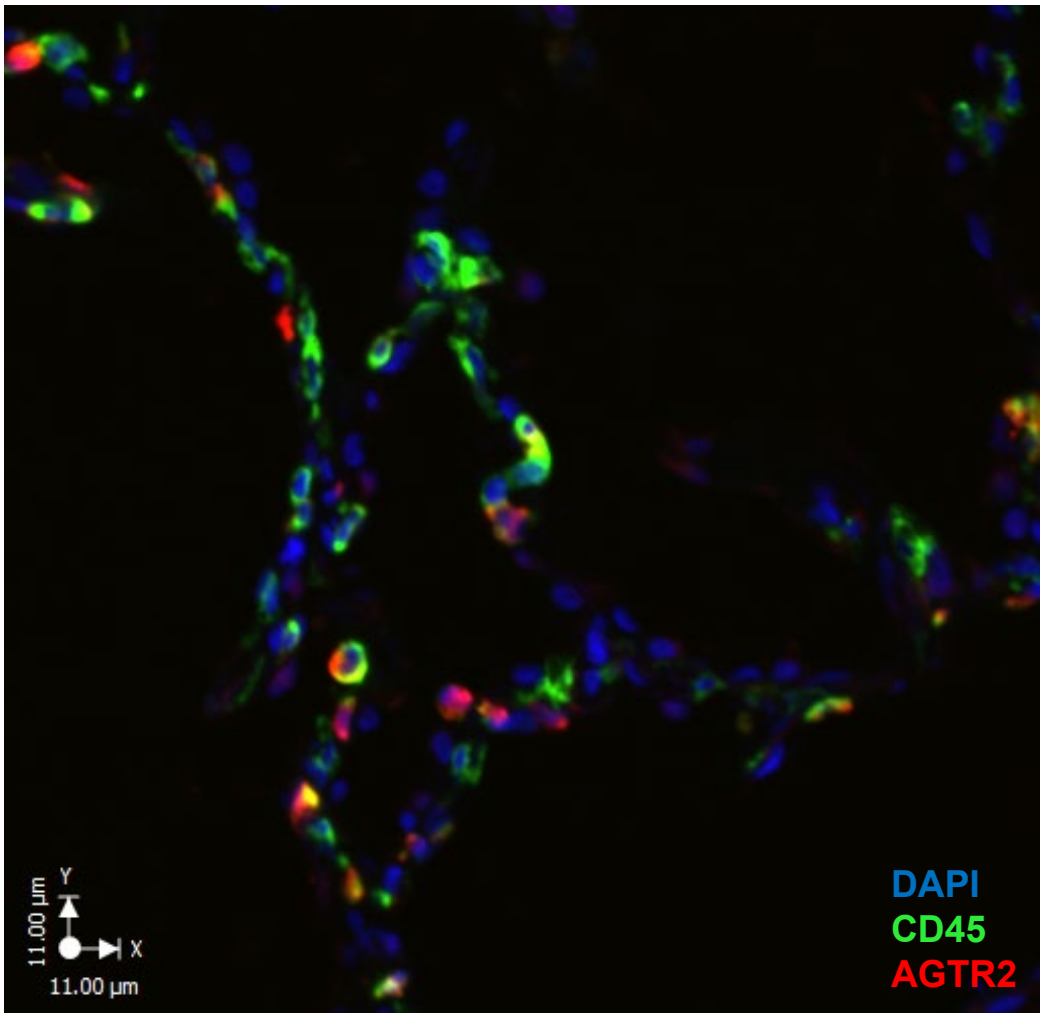
DAPI
CD45
AGTR2
Y
11.00 µm
X
11.00 µm

Supplemental Figure S5: AngII receptor transcripts in lung tissue.

AngII receptor transcripts in CLAD (RAS and BOS) and control lung samples. (A) Levels of AGTR1 transcripts in lung samples, adjusted for the housekeeping gene *PPIA*. (B) AGTR2 transcripts in lung samples, adjusted for the housekeeping gene *PPIA*. (C) Ratio of the AGTR1-to-AGTR2 transcripts.

S5

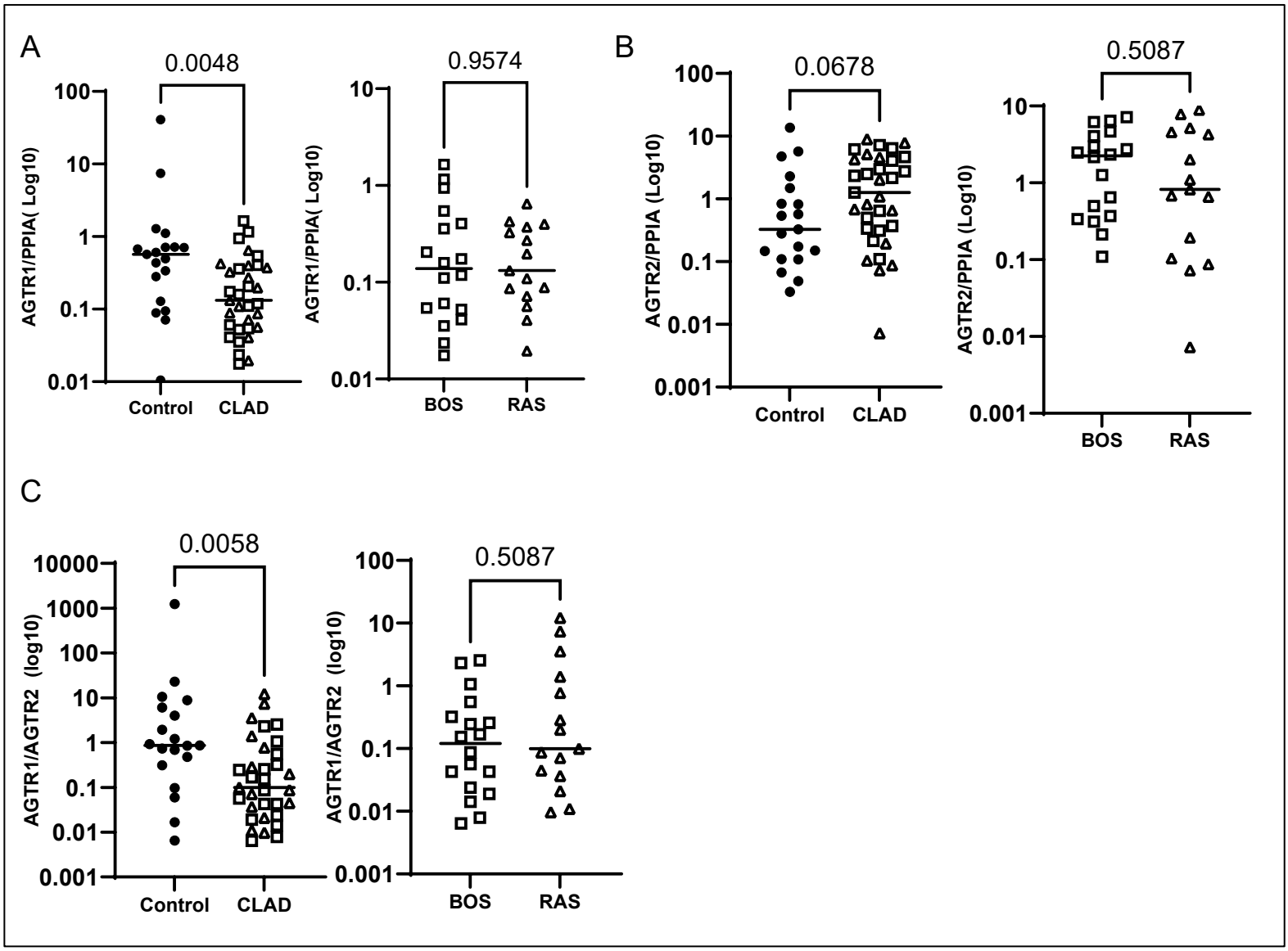
A
0.0048
AGTR1/PPIA(Log10)
100
10
1
0.1
0.01
Control
CLAD
0.9574
AGTR1/PPIA(Log10)
10
1
0.1
0.01
BOS
RAS
B
0.0678
AGTR2/PPIA (Log10)
100
10
1
0.1
0.01
0.001
Control
CLAD
0.5087
AGTR2/PPIA (Log10)
10
1
0.1
0.01
0.001
BOS
RAS
C
0.0058
AGTR1/AGTR2 (log10)
10000
1000
100
10
1
0.1
0.01
0.001
Control
CLAD
0.5087
AGTR1/AGTR2 (log10)
100
10
1
0.1
0.01
0.001
BOS
RAS

Supplemental Figure S6: RT-qPCR Melting curves.

(A) The melting curves of RT-qPCR for AGTR1, (B) AGTR2, (C) TSP1, (D) GLNA, (E) LYPA1, (F) and BST1 are presented in this figure. *LYPA1, Lysophospholipase 1; BST1, Bone Marrow Stromal Cell Antigen 1; GLNA (=GLUL official transcript name), Glutamine Synthetase; TSP1 (=THBS1 official transcript name), Thrombospondin; AGTR1, Angiotensin II type I receptor; AGTR2, Angiotensin II type II receptor; CLAD, Chronic lung allograft dysfunction.*

S6 (1/2)

A

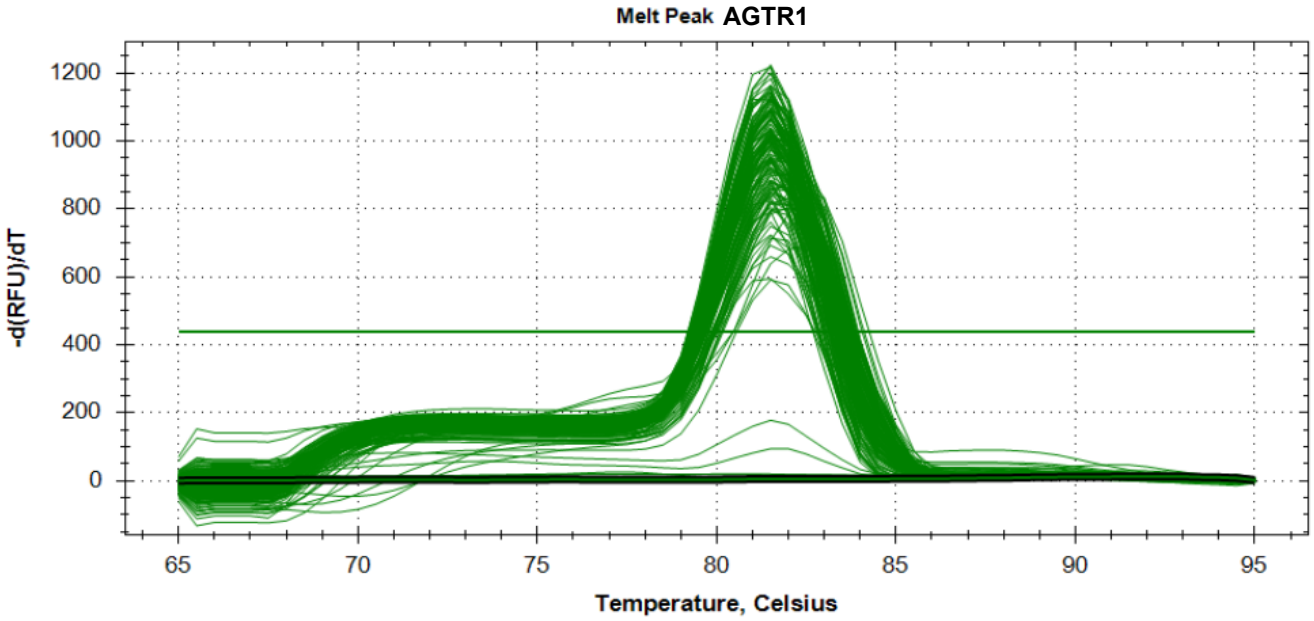
Melt Peak AGTR1
-d(RFU)/dT
1200
1000
800
600
400
200
0
65
70
75
80
85
90
95
Temperature, Celsius

B

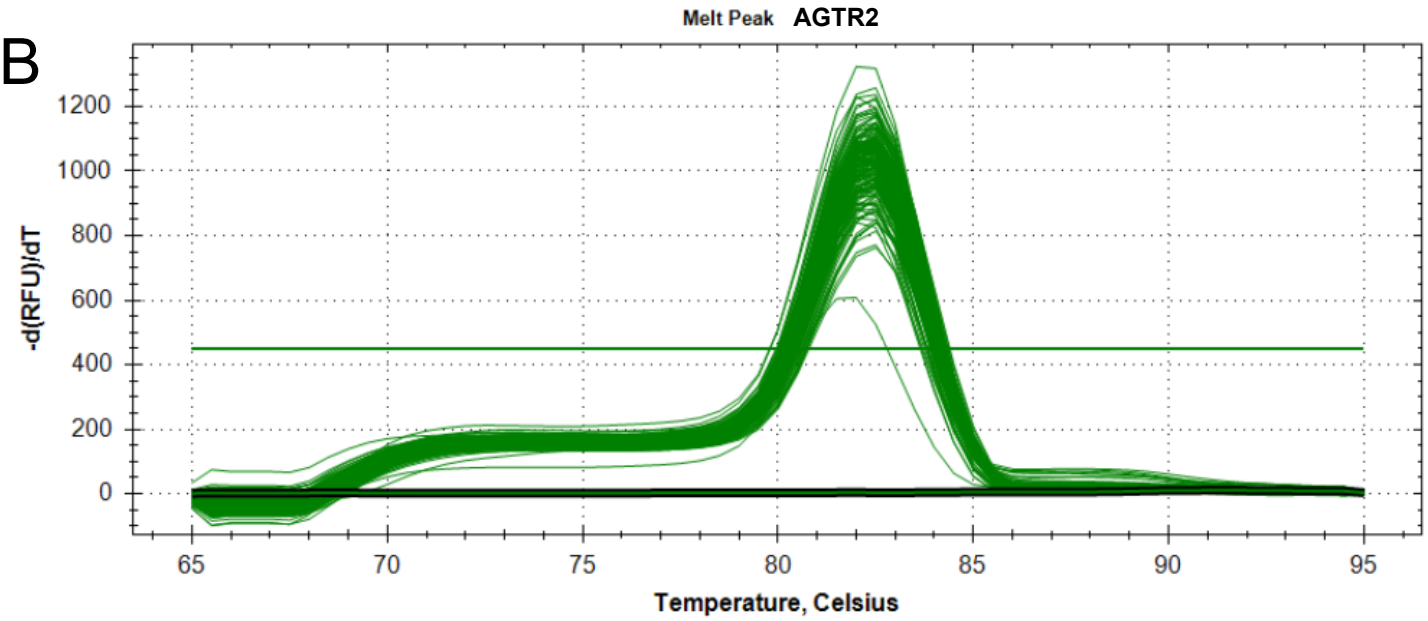
Melt Peak AGTR2
-d(RFU)/dT
1200
1000
800
600
400
200
0
65
70
75
80
85
90
95
Temperature, Celsius

C

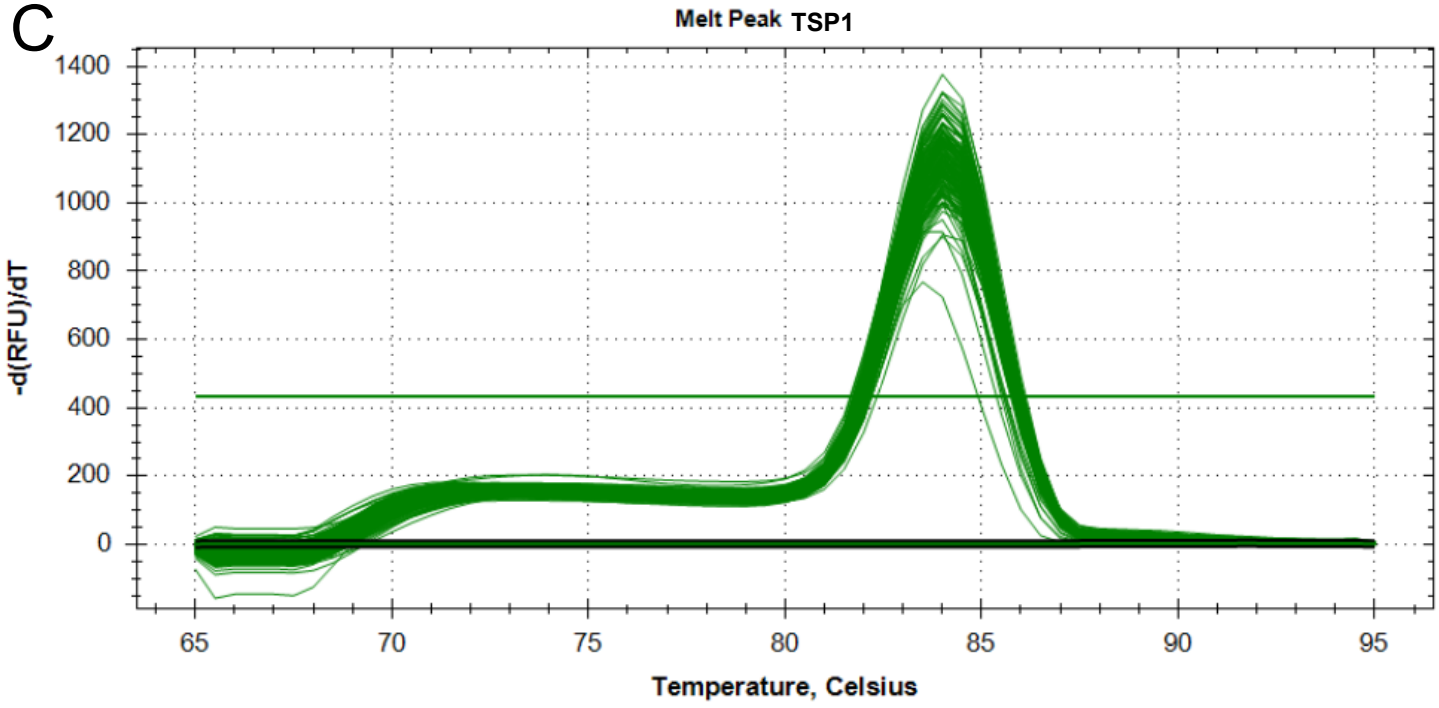
Melt Peak TSP1
-d(RFU)/dT
1400
1200
1000
800
600
400
200
0
65
70
75
80
85
90
95
Temperature, Celsius

S6 (2/2)

D

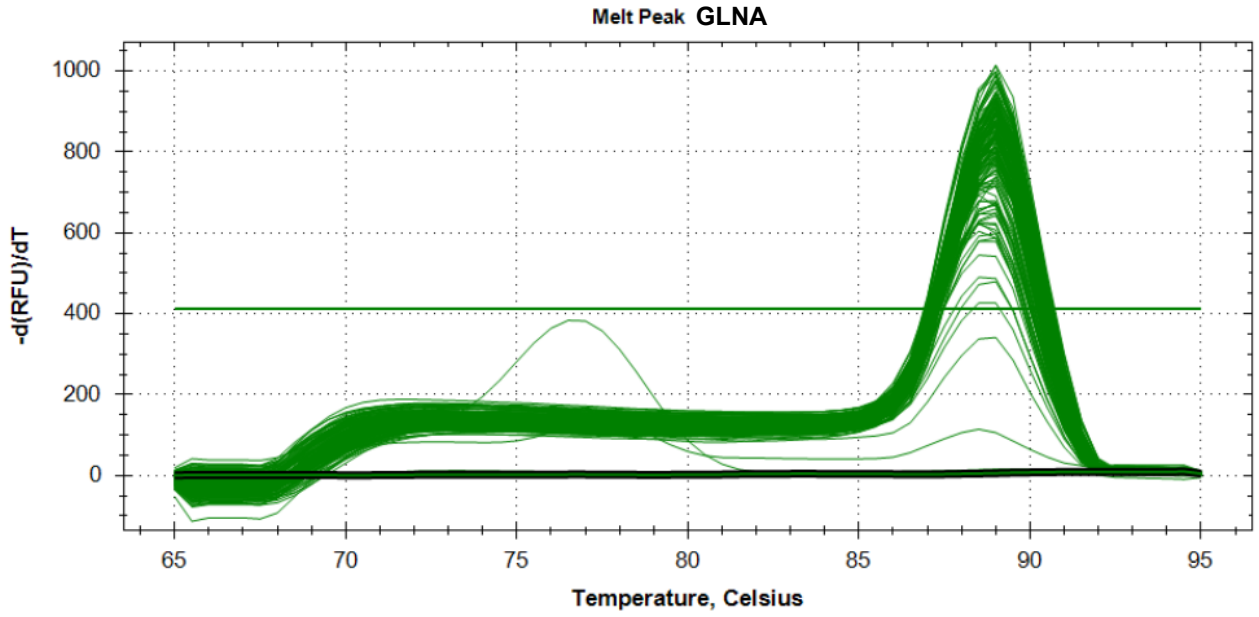
Melt Peak GLNA
-d(RFU)/dT
1000
800
600
400
200
0
65
70
75
80
85
90
95
Temperature, Celsius

E

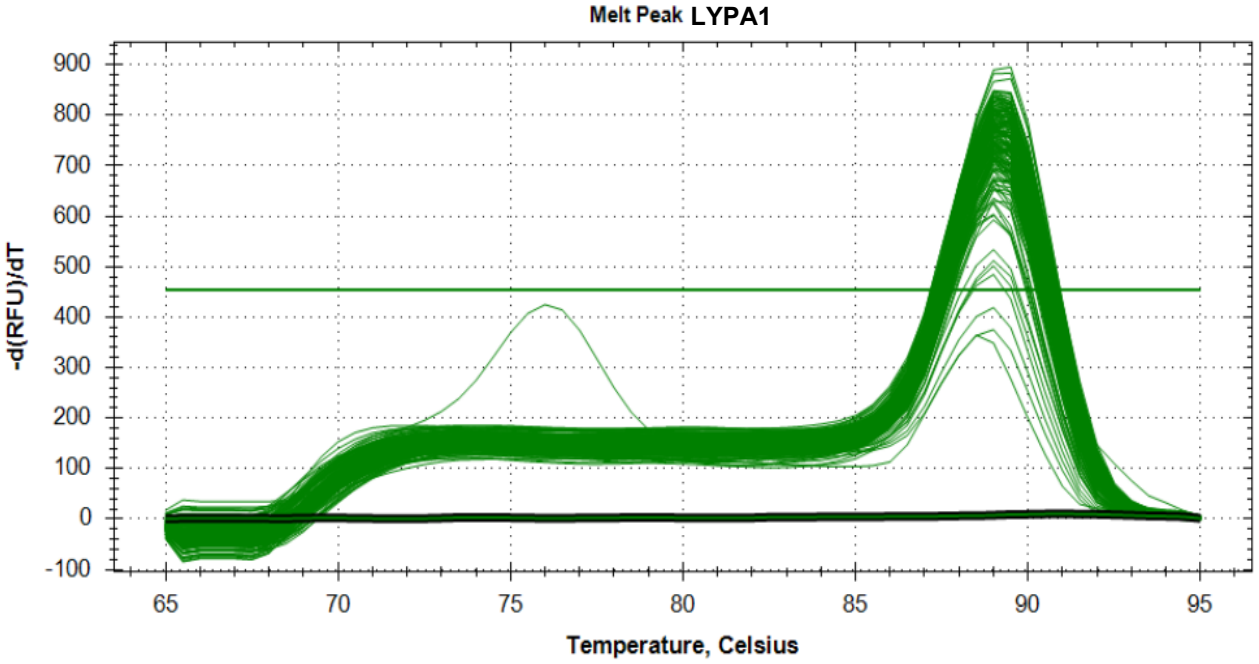
Melt Peak LYPA1
-d(RFU)/dT
900
800
700
600
500
400
300
200
100
0
-100
65
70
75
80
85
90
95
Temperature, Celsius

F

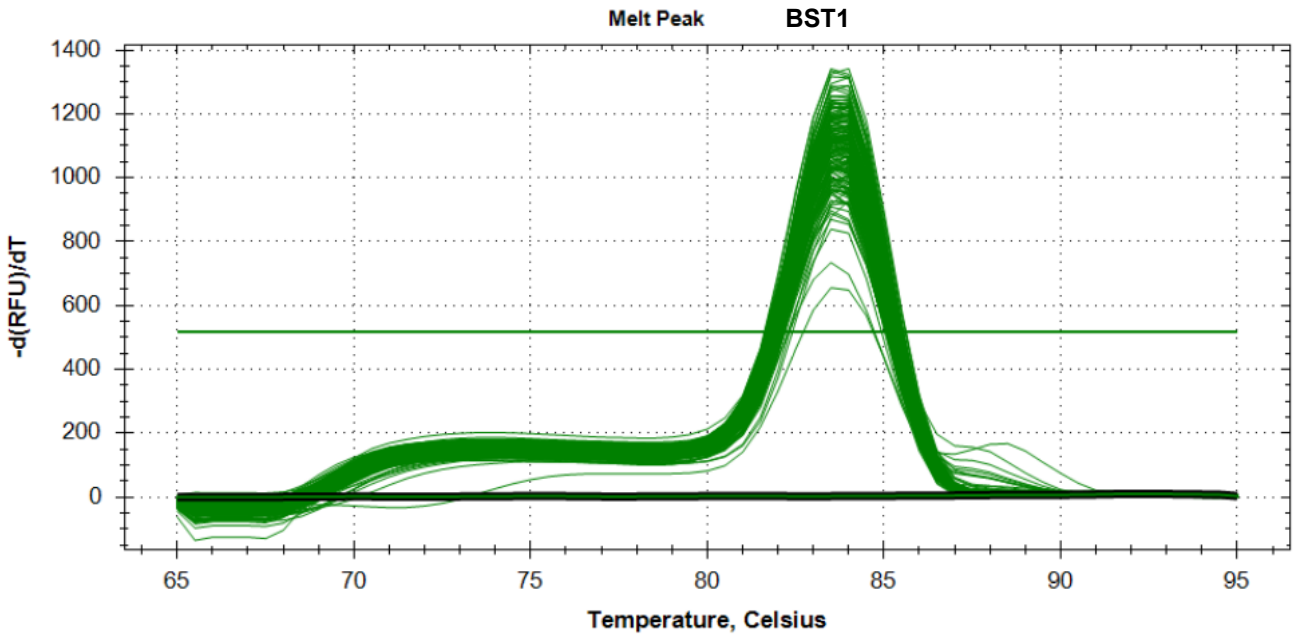
Melt Peak BST1
-d(RFU)/dT
1400
1200
1000
800
600
400
200
0
65
70
75
80
85
90
95
Temperature, Celsius

Supplemental Figure S7: Migration of gene amplicons on agarose gel.

This figure shows the migration on agarose gel of the amplicons of the 6 genes tested in Supplemental Figure 13: AGTR1, AGTR2, TSP1, GLNA, BST1, and LYPA1. (A and B) Two different images were taken to adequately capture the whole gel. The two different exposure times show that there is only one band per transcript. Of note, there is no amplicon of AGTR2 in the skin, but this is consistent with the information provided on the proteinatlas.org. *LYPA1, Lysophospholipase 1; BST1, Bone Marrow Stromal Cell Antigen 1; GLNA (=GLUL official gene name), Glutamine Synthetase; TSP1 (=THBS1 official gene name), Thrombospondin; AGTR1, Angiotensin II type I receptor; AGTR2, Angiotensin II type II receptor; CLAD, Chronic lung allograft dysfunction.*

S7

A

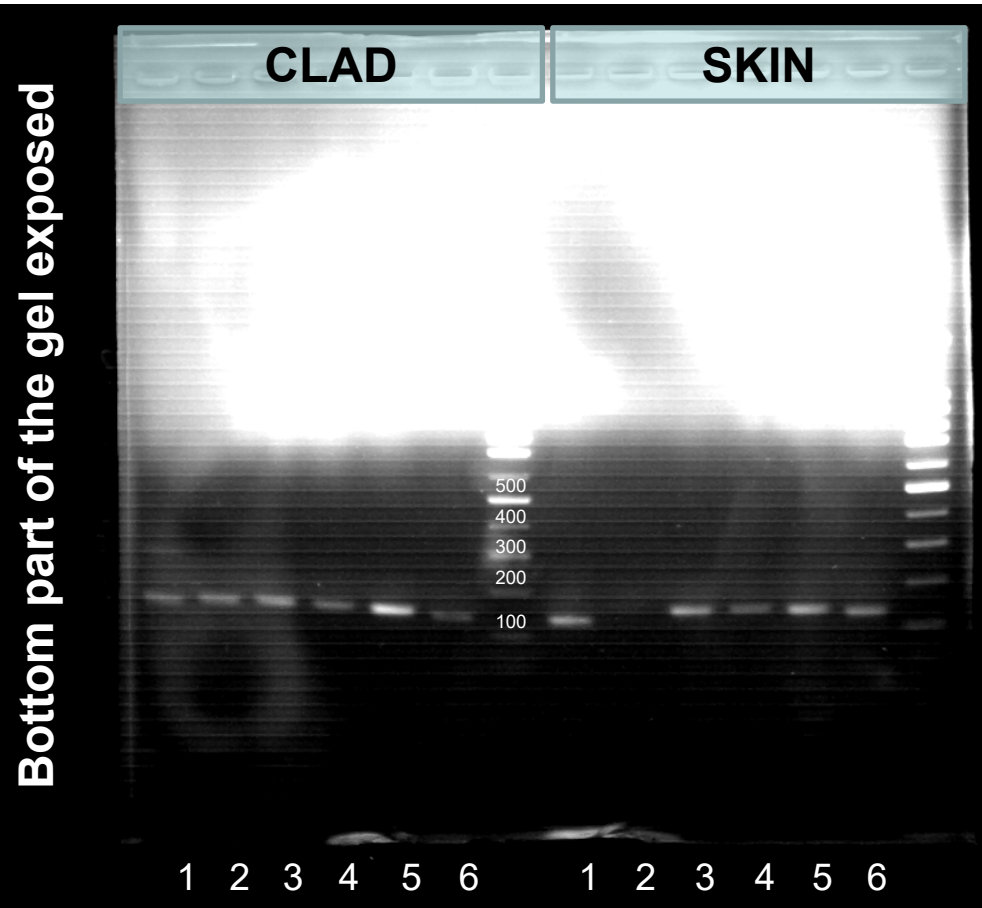

1. AGTR1
2. AGTR2
3. TSP1
4. GLNA
5. BST1
6. LYPA1

B

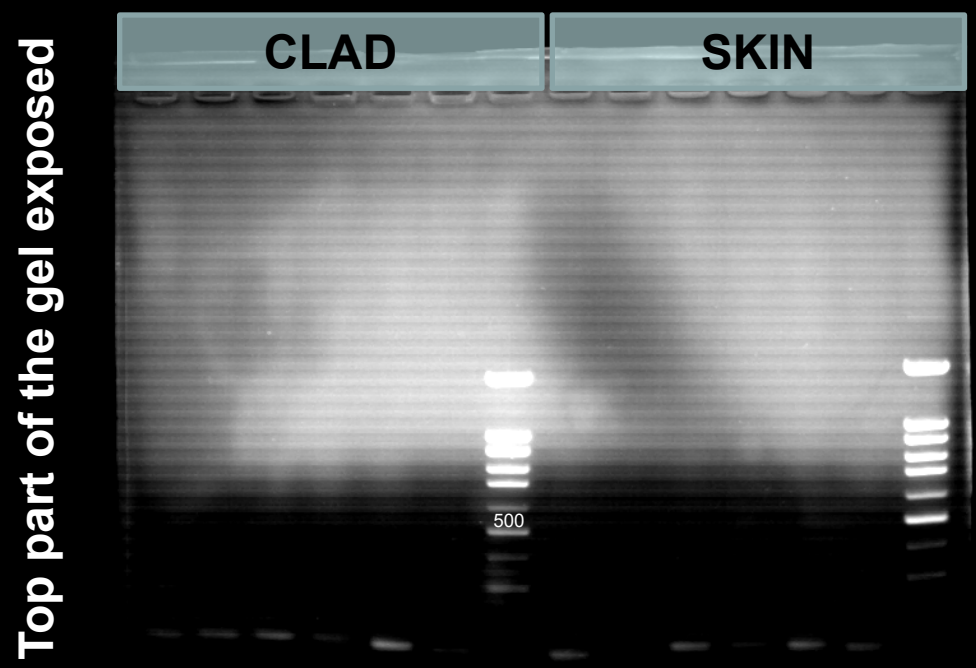

Supplemental Figure S8: TSP1 and GLNA immunostaining controls.

(A) Positive staining and secondary antibody only for TSP1 and GLNA in human kidney. (B) Positive staining and secondary antibody only of TSP1 and GLNA in human CLAD lungs. *TSP1, thrombospondin 1; GLNA, glutamine synthetase.*

TSP1, thrombospondin 1; GLNA, glutamine synthetase; CLAD, Chronic lung allograft dysfunction.

S8

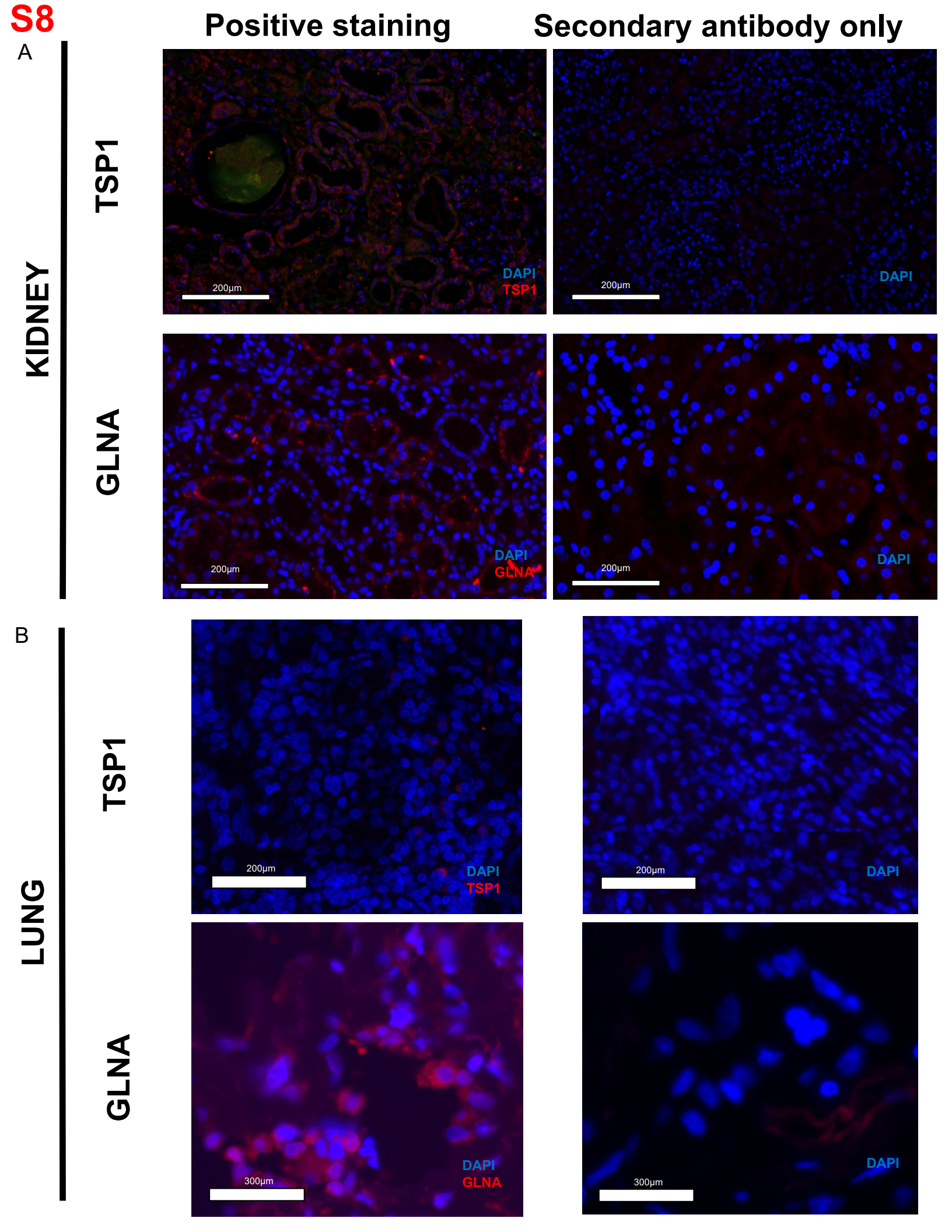
Positive staining
Secondary antibody only
A
KIDNEY
TSP1
GLNA
DAPI
TSP1
DAPI
GLNA
200µm
B
LUNG
300µm

Supplemental Figure S9: Representative immunohistochemistry staining patterns and secondary antibody only staining for TSP1 and GLNA in human CLAD lungs.

(A, B) Positive immunohistochemistry staining patterns of TSP1, and (C, D) GLNA are shown in different representative zones of CLAD pathology. (A) Typical bronchiolitis obliterans lesion, (B, C, D) parenchymal fibrosis, (C, D) alveolar region. The panels on the right are the corresponding secondary antibody only staining. *TSP1, thrombospondin 1; GLNA, glutamine synthetase; CLAD, Chronic lung allograft dysfunction.*

S9

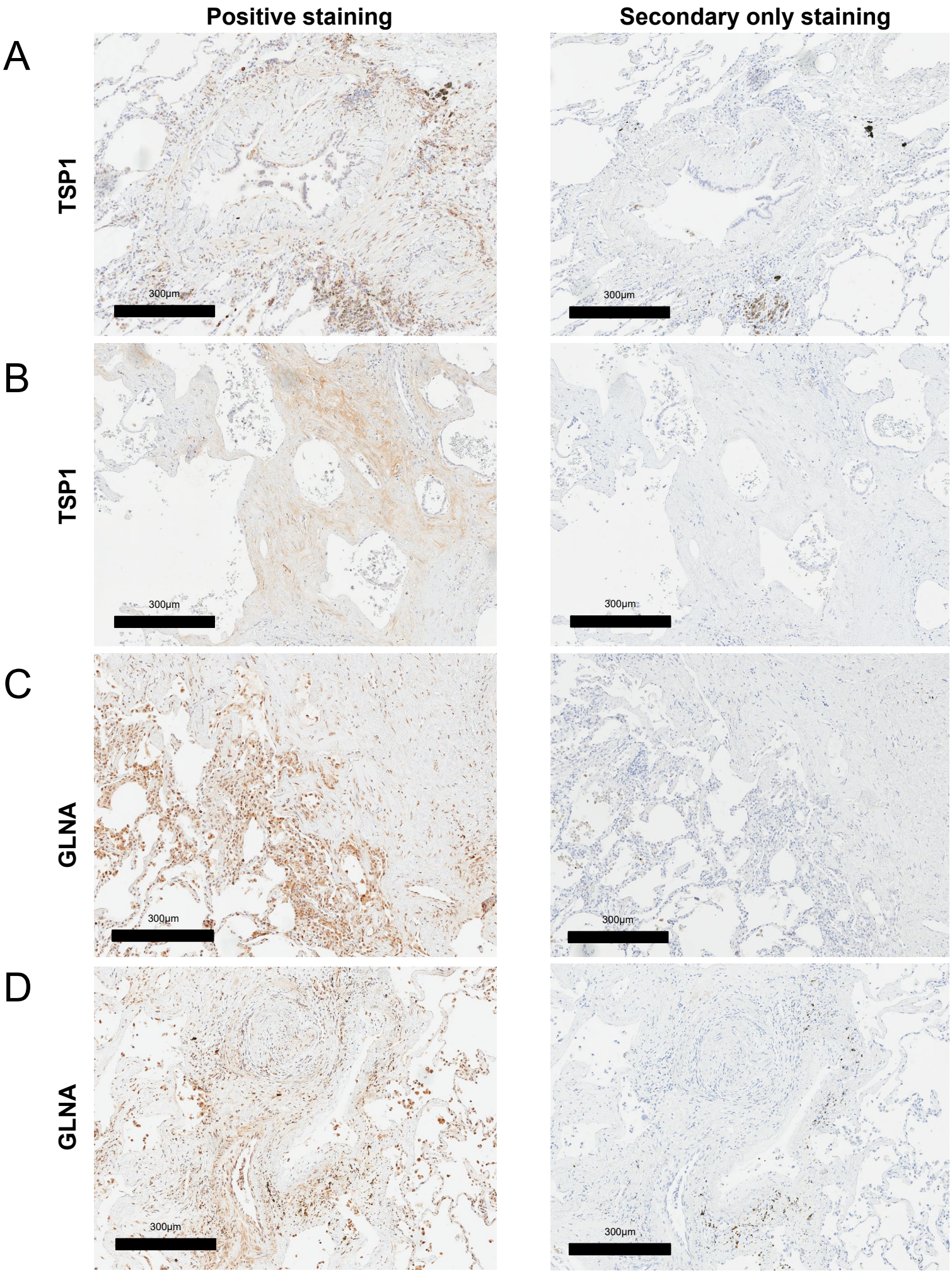
Positive staining
Secondary only staining
A
TSP1
300µm
300µm
B
TSP1
300µm
300µm
C
GLNA
300µm
300µm
D
GLNA
300µm
300µm

Supplemental Figure 10: GLNA and TSP1 quantification in lung tissue by Western blot.

(A) Western blot analysis of GLNA protein and housekeeping protein vinculin in 4 control lung samples and 4 CLAD (RAS) samples. Dot plot represents the densitometric readings for GLNA adjusted for vinculin. (B) Western blot analysis of TSP1 protein and housekeeping protein GAPDH in 4 control lung samples versus 4 CLAD samples. Dot plot represents densitometric readings for TSP1 adjusted for GAPDH. In both cases P was calculated with Mann-Whitney test. *RAS, restrictive allograft syndrome; GLNA, glutamine synthetase; TSP1, thrombospondin 1; GAPDH, glyceraldehyde-3-phosphate dehydrogenase*.

S10A

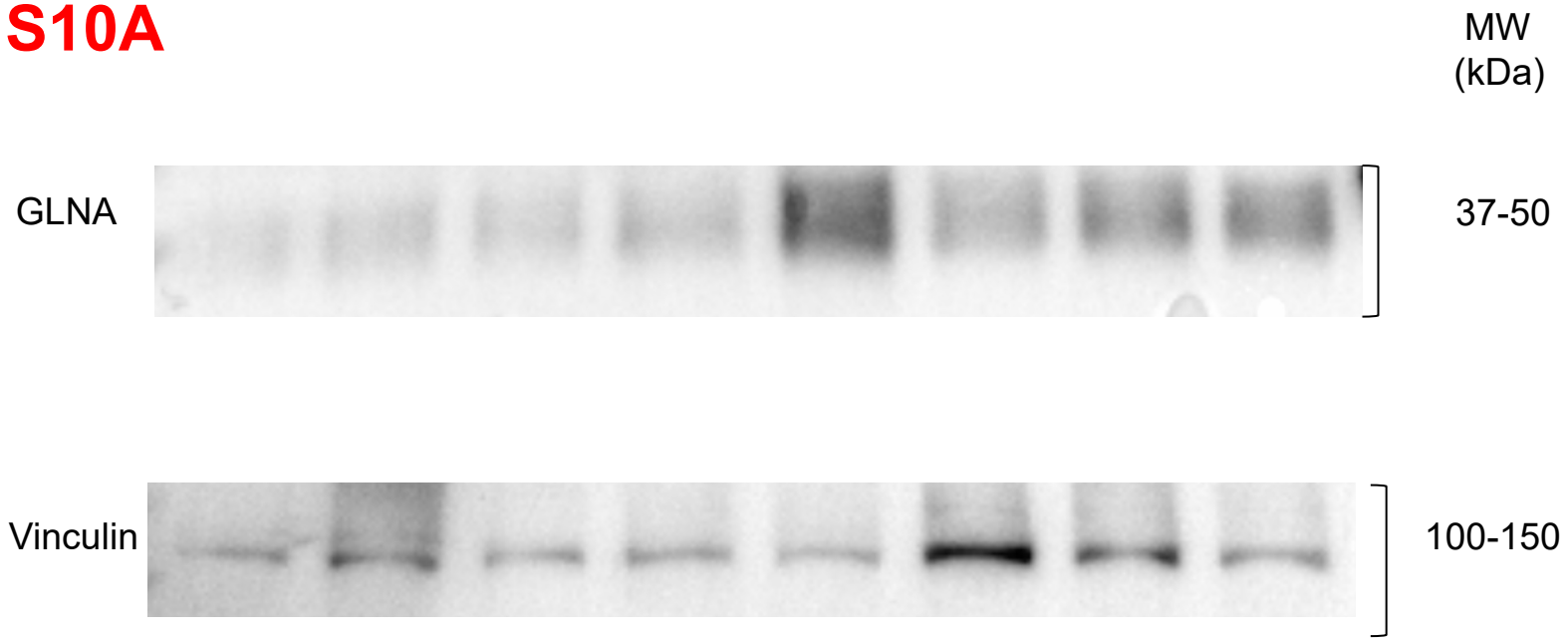
MW
(kDa)
GLNA
37-50
Vinculin
100-150
Control lungs
CLAD samples

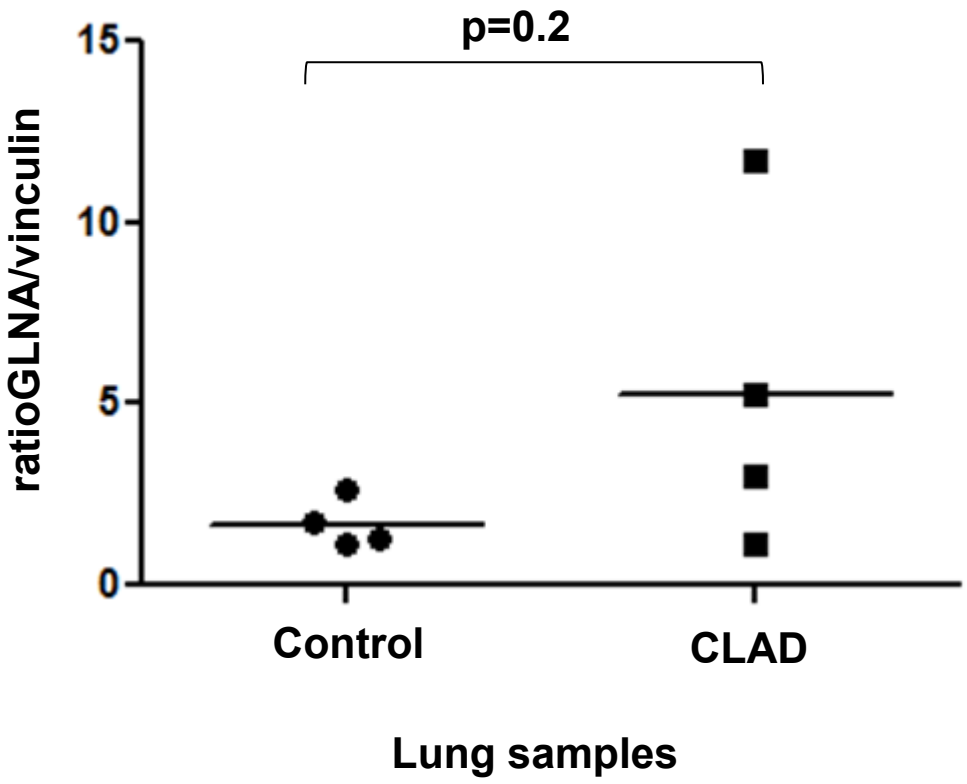
p=0.2
15
10
5
0
ratioGLNA/vinculin
Control
CLAD
Lung samples

S10B

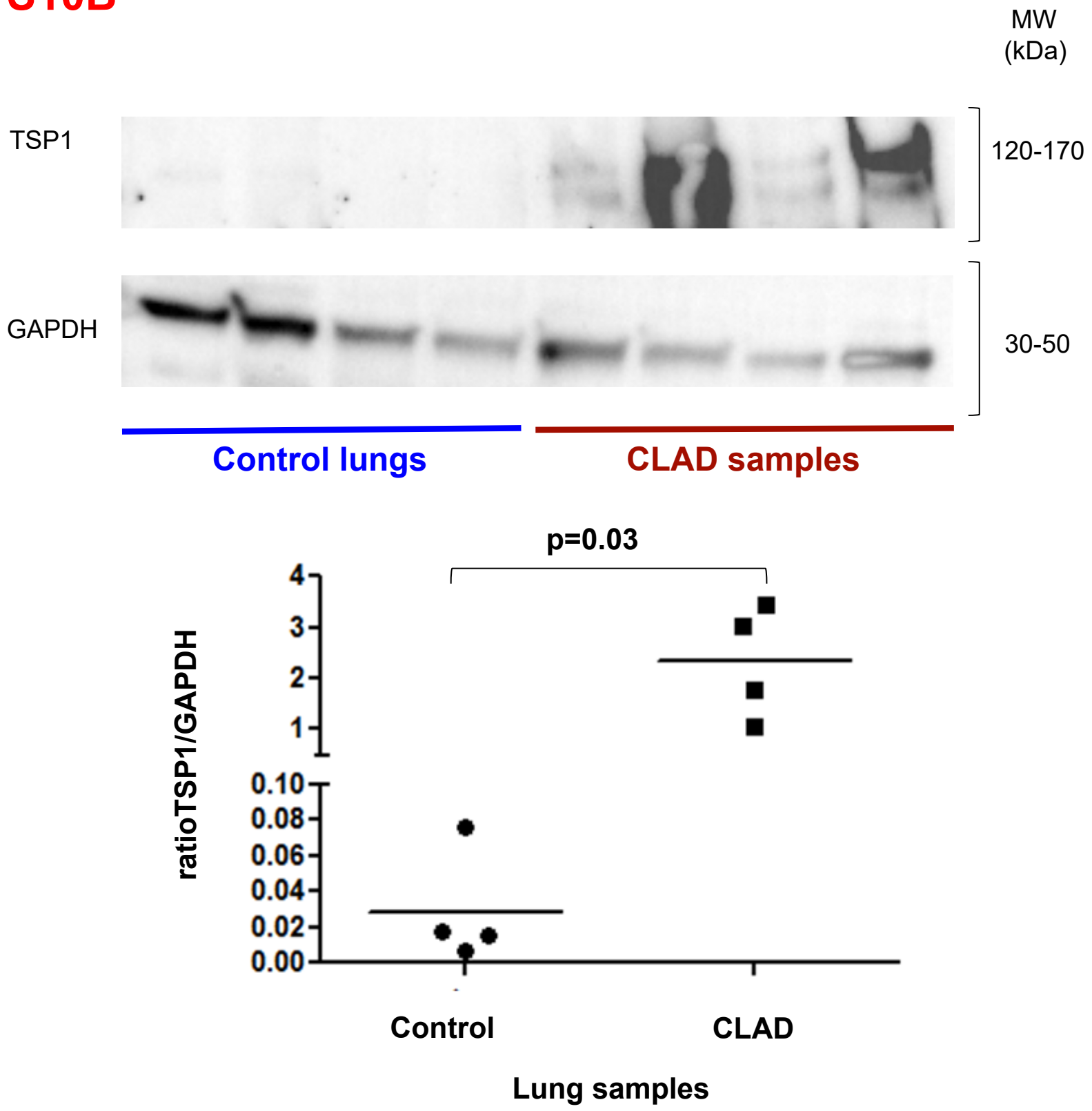
MW
(kDa)
TSP1
120-170
GAPDH
30-50
Control lungs
CLAD samples
p=0.03
ratioTSP1/GAPDH
4
3
2
1
0.10
0.08
0.06
0.04
0.02
0.00
Control
CLAD
Lung samples

Supplemental Figure S11: Monocytes/Macrophages express TSP1 and GLNA in lung tissue.

(A) TSP1 (in red) co-staining with CD68 (in green). (B) GLNA (in red) co-staining with CD68 (in green). (C) GLNA (in red) co-staining with panCK (in green). These panels show co-staining of TSP1 and GLNA with CD68, suggesting expression of these proteins by monocytes/macrophages. GLNA immunostaining can also be seen, to a lesser degree, in panCK positive lung epithelial cells. *TSP1, thrombospondin 1; GLNA, glutamine synthetase; panCK, pan-cytokeratin.*

S11

A

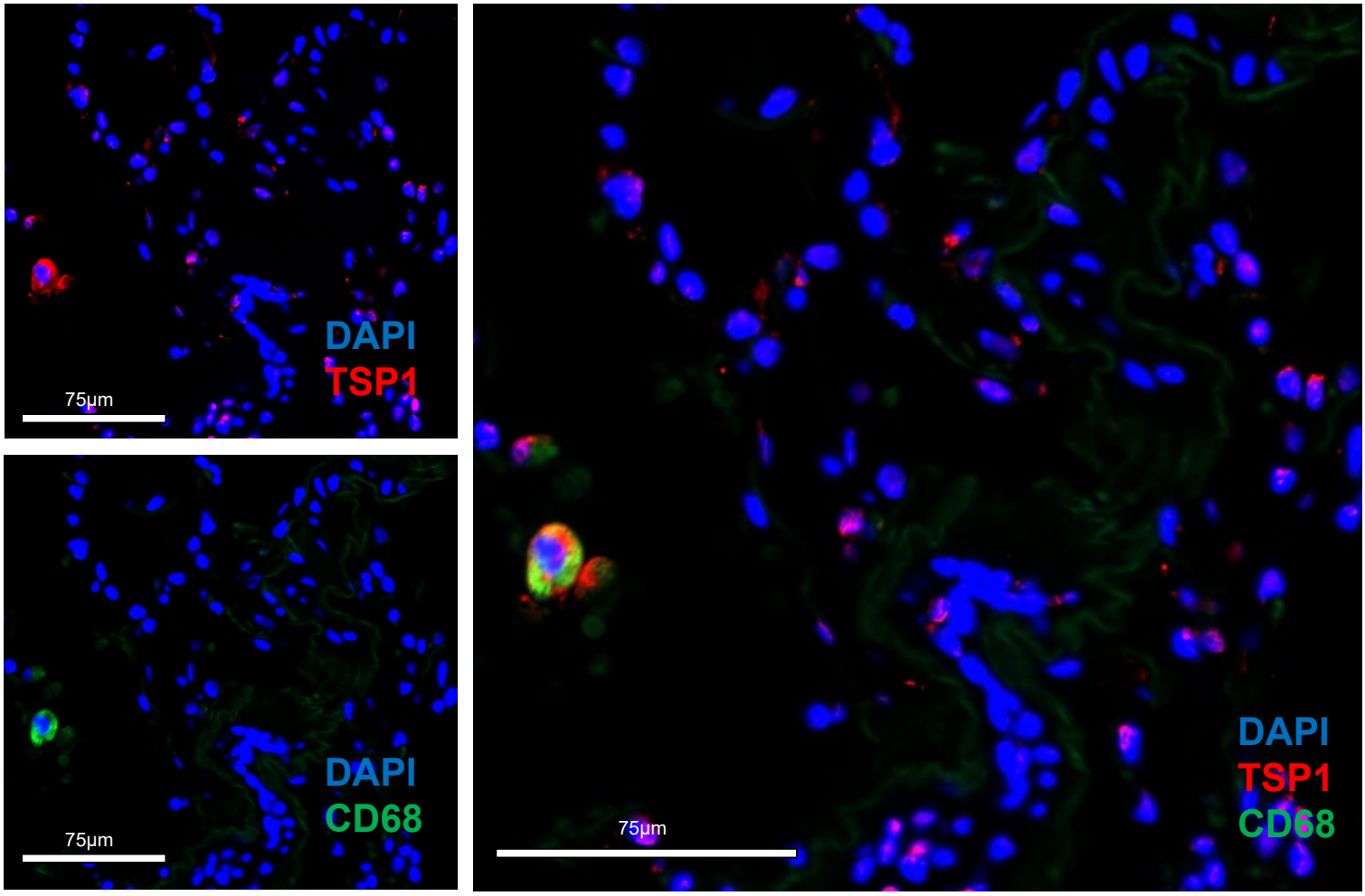
DAPI
TSP1
75μm
DAPI
CD68
75μm
DAPI
TSP1
CD68
75μm

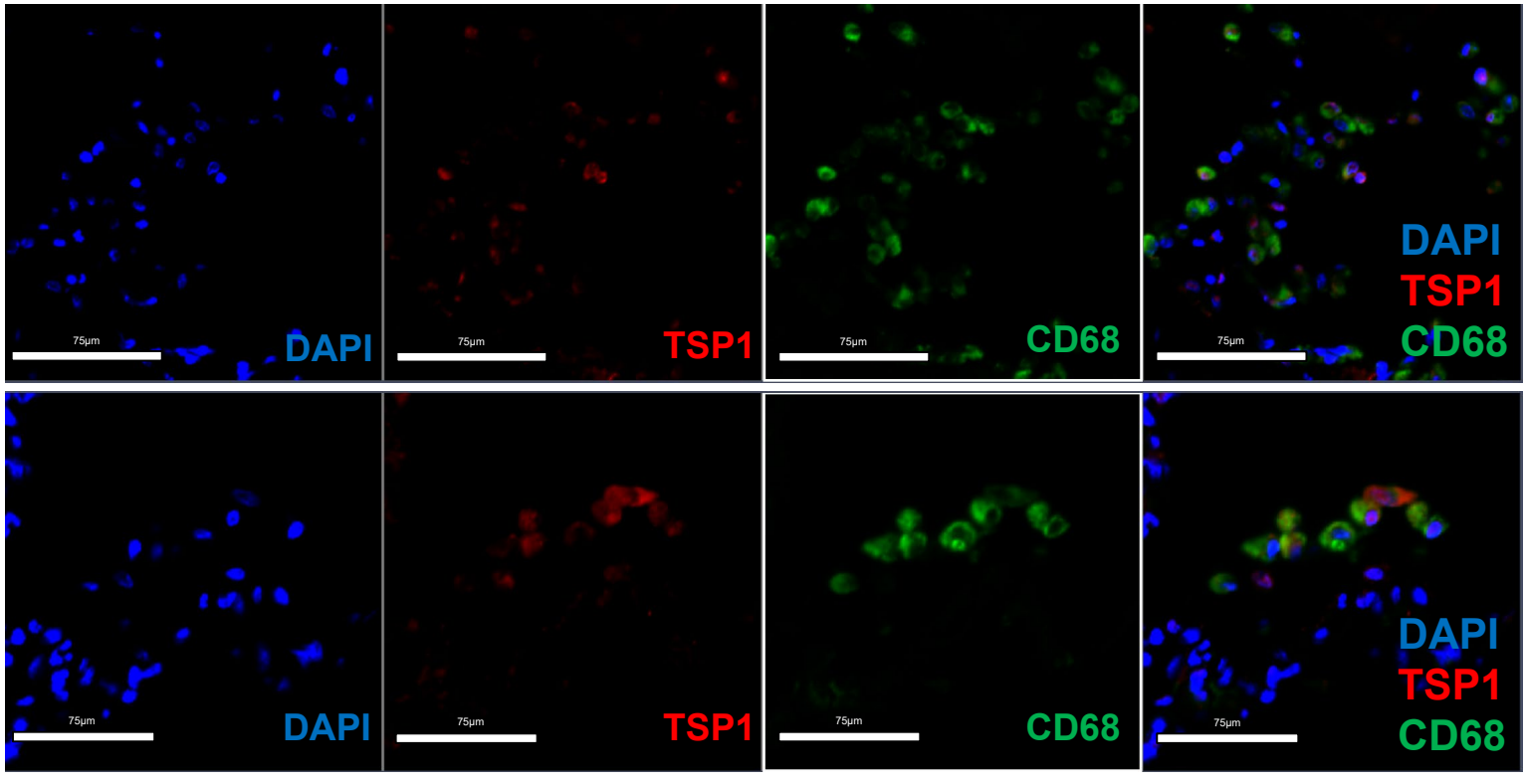
75μm
DAPI
75μm
TSP1
75μm
CD68
75μm
DAPI
TSP1
CD68
75μm
DAPI
75μm
TSP1
75μm
CD68
75μm
DAPI
TSP1
CD68

S11

B

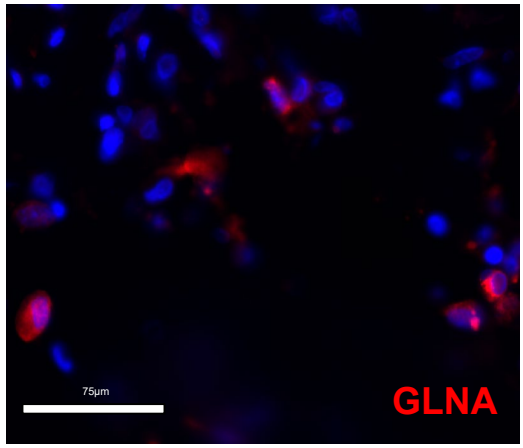
75μm
GLNA

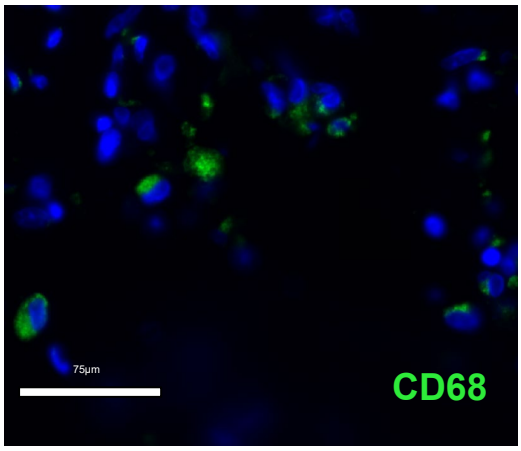
75μm
CD68

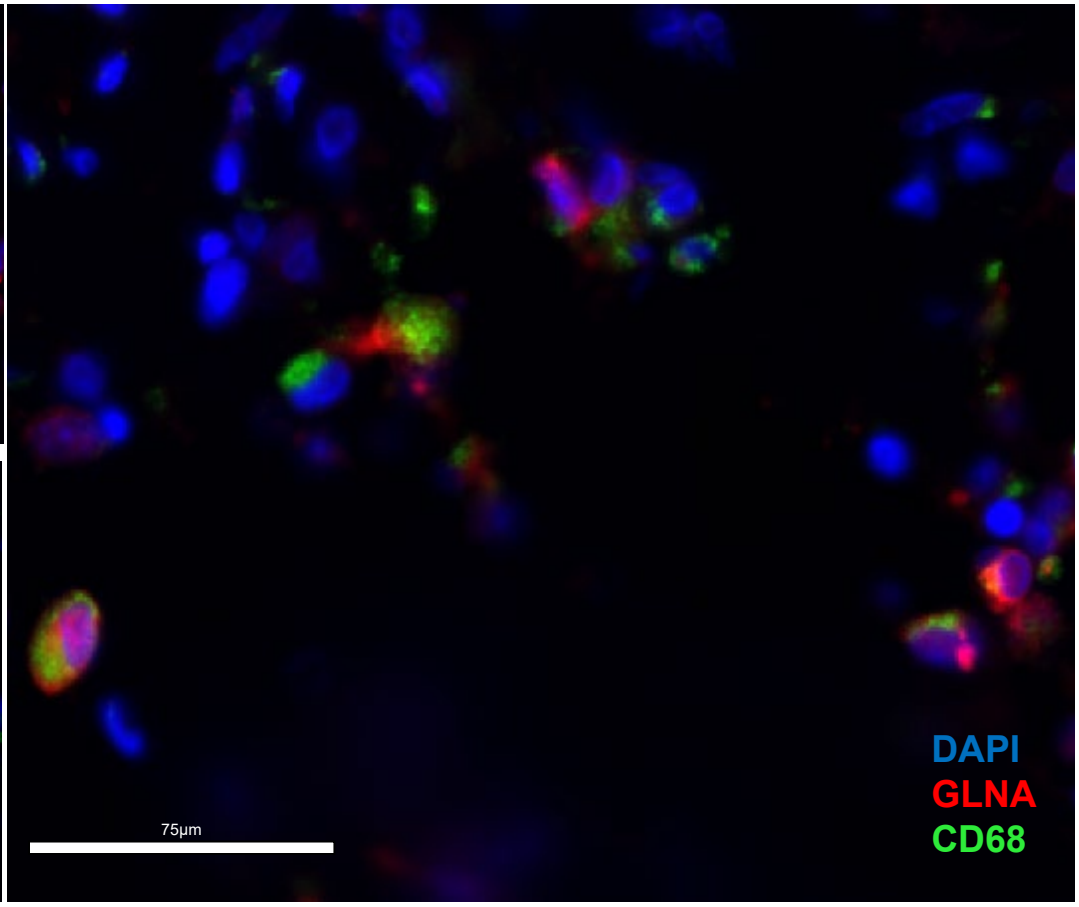
75μm
DAPI
GLNA
CD68

C

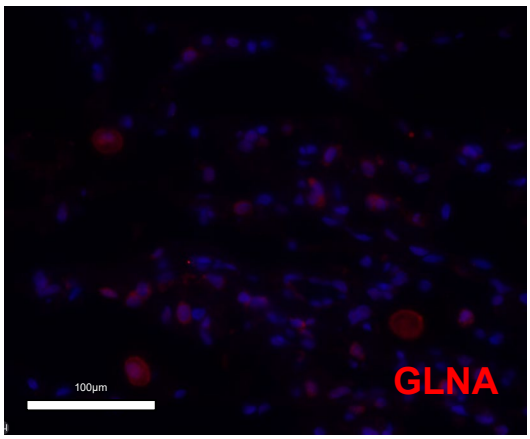
100μm
GLNA

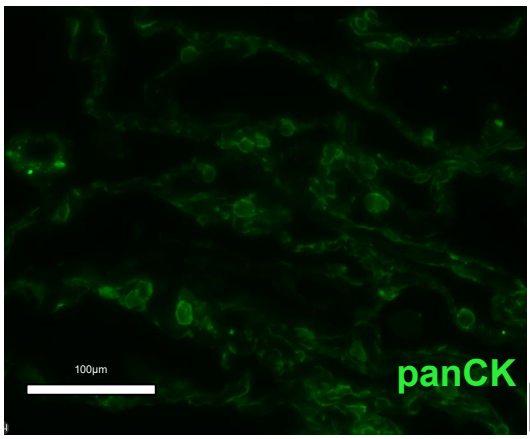
100μm
panCK

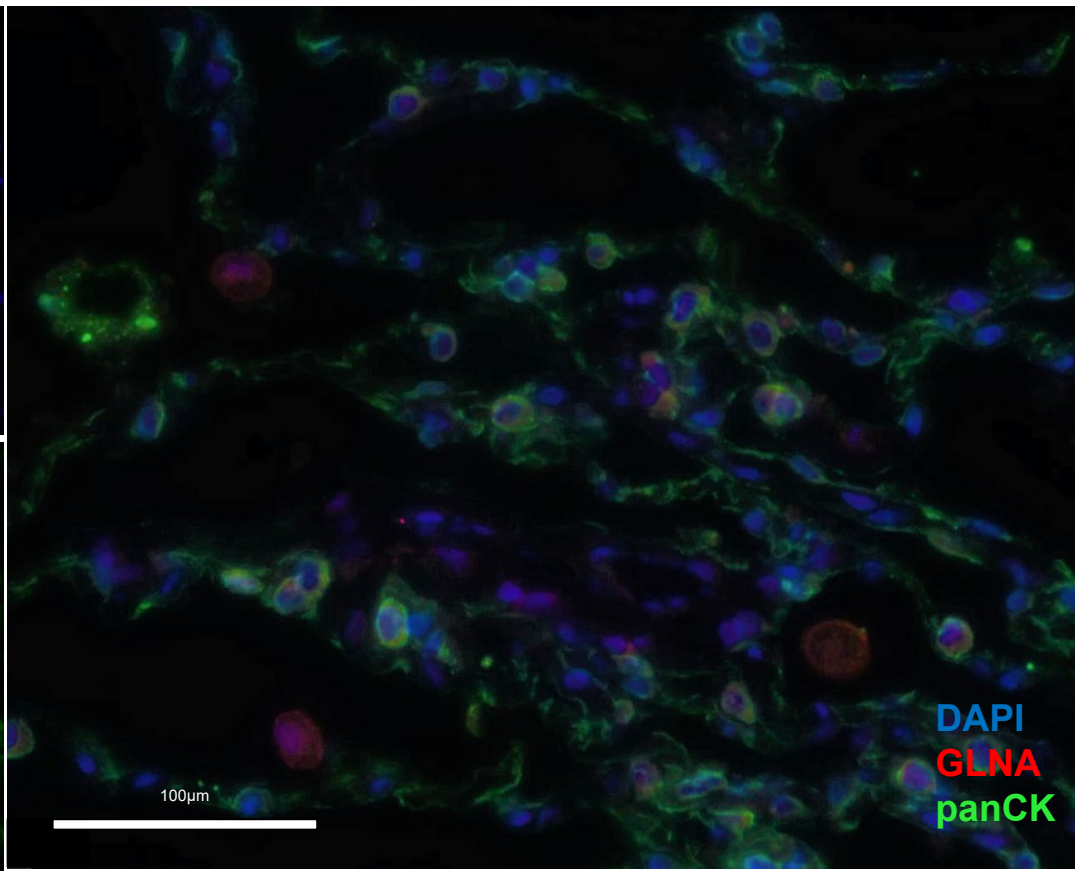
100μm
DAPI
GLNA
panCK

Supplemental Figure S12: Semi-quantitative scoring system for immunostaining of AngII-regulated proteins.

A blinded scoring system was used for evaluation of immunohistochemistry slides stained for TSP1 (A) or GLNA (B). Representative images of each grade are shown. *TSP1, thrombospondin 1; GLNA, glutamine synthetase.*

S12

A **TSP1 staining scale: surface and intensity**

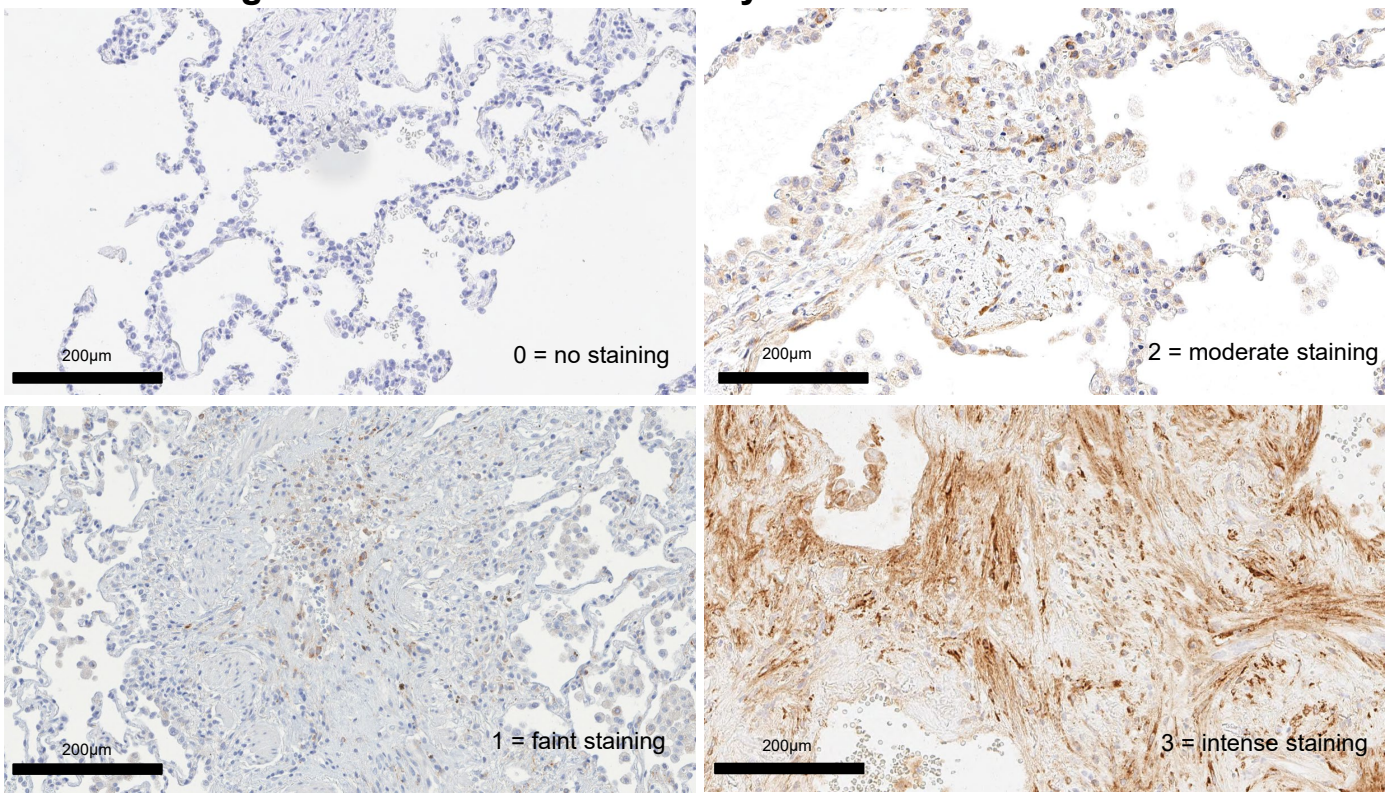

B **GLNA staining scale: number of positive cells and intensity**

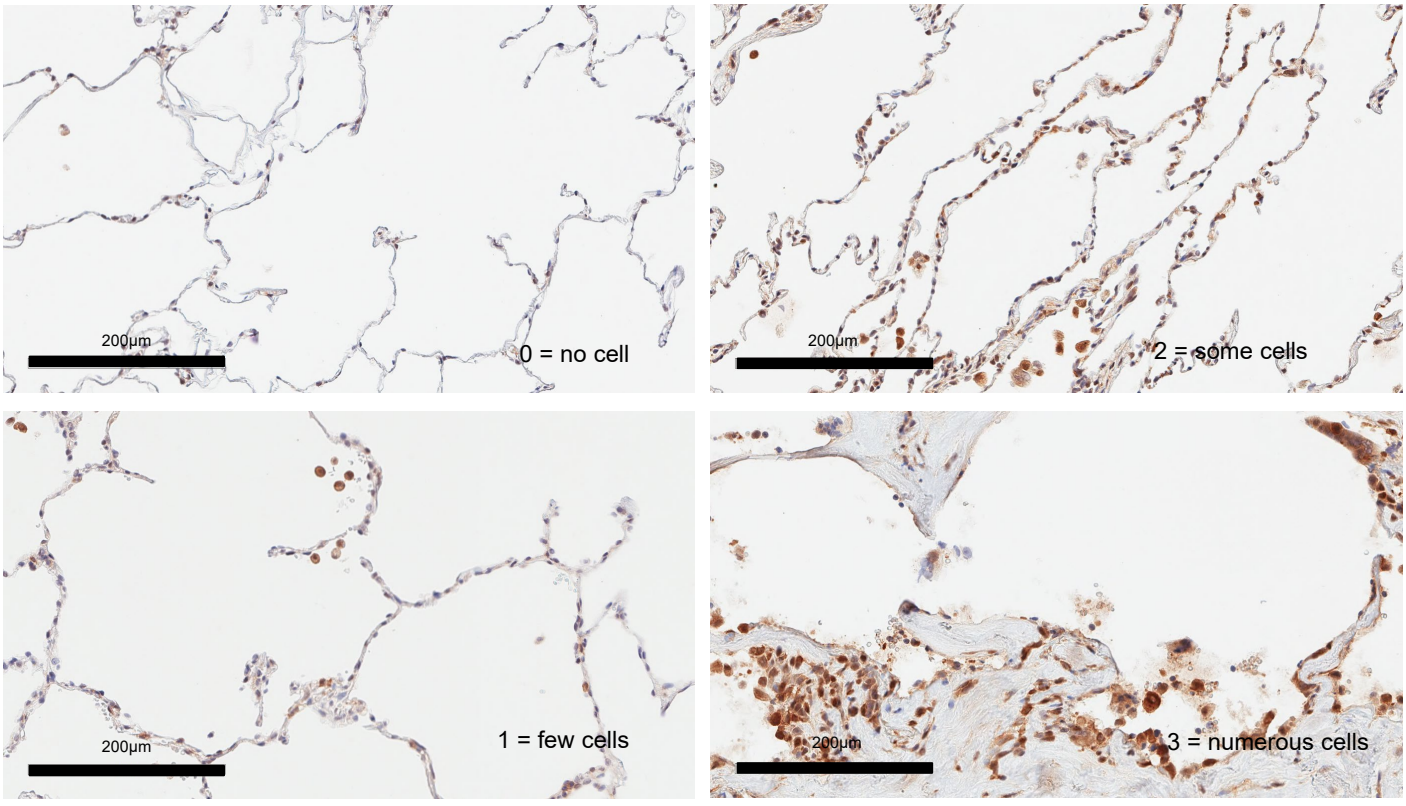

Supplemental Figure S13: AngII-regulated protein transcripts in lung tissue.

Gene expression of AngII-regulated proteins in CLAD and control lung samples. (A) Transcript levels of LYPA1 transcripts, adjusted for the housekeeping gene *PPIA*. (B) Transcript levels of BST1, adjusted for the housekeeping gene *PPIA*. *LYPA1, lysophospholipase 1; BST1, bone marrow stromal cell antigen 1.*

S13

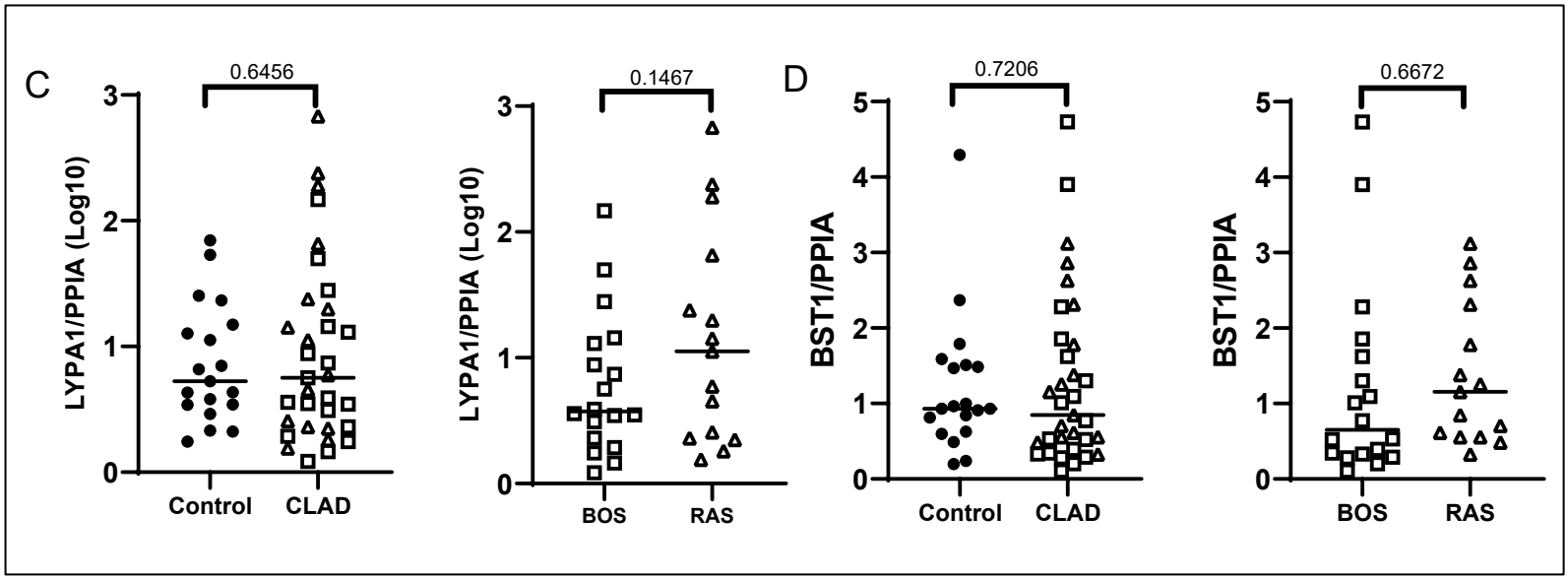
C
0.6456
LYPA1/PPIA (Log10)
3
2
1
0
Control
CLAD
0.1467
LYPA1/PPIA (Log10)
3
2
1
0
BOS
RAS
D
0.7206
BST1/PPIA
5
4
3
2
1
0
Control
CLAD
0.6672
BST1/PPIA
5
4
3
2
1
0
BOS
RAS

Supplemental Figure S14: Optimization of normalized collision energy (NCE) for each precursor peptide for PRM analysis.

The optimization of the energy applied for collision-induced fragmentation and subsequent production of fragments (transitions) from the selected peptides can enhance the sensitivity of each PRM assay. Optimal NCE was experimentally defined for each precursor peptide. Several values of NCE (18, 21, 24, 27, 30, 33) were set using Q-Exactive™ Plus software and the signal produced by each peptide was monitored. Each bar graph shows the raw peak areas acquired for each peptide, with the x-axis showing the NCE applied for each replicate. Each colour in each bar represents the signal contributed from individual transitions. Optimal NCE corresponding to the greatest peak area for each peptide was selected. *PRM, Parallel reaction monitoring; NCE, Normalized collision energy*.

S14

GGVNDNFQGVLQNVR

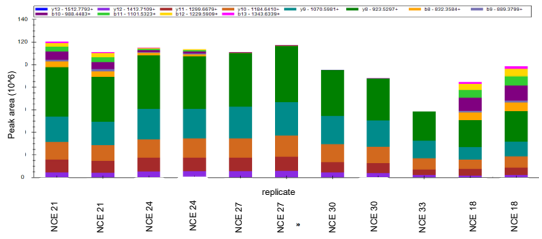

TSP1

TIVTTLQDSIR

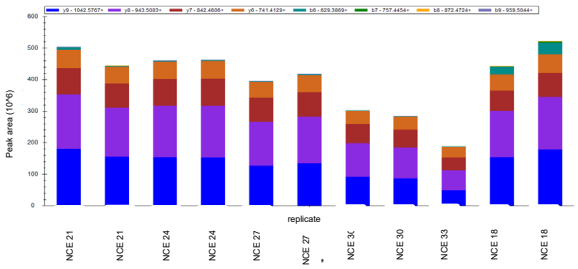

ALLSPEQR

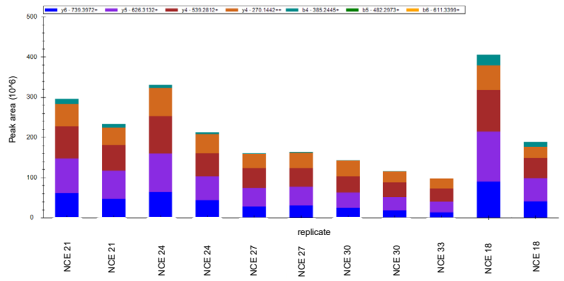

BST1

GFFADYEIPNLQK

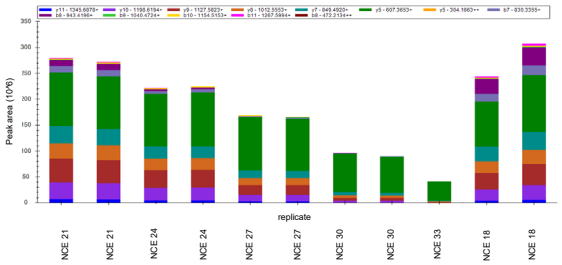

GLNA

LVLCEVFK

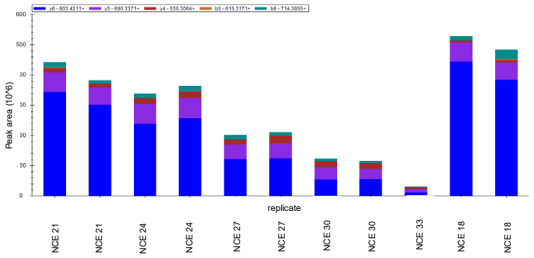

DIVEAHYR

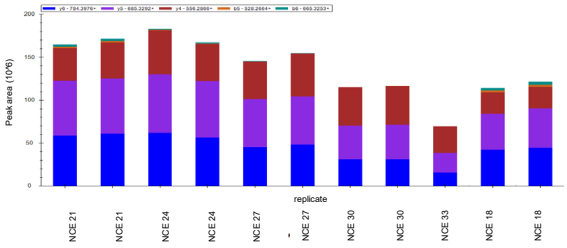

LAMB2

GSCYPATGDLLVGR

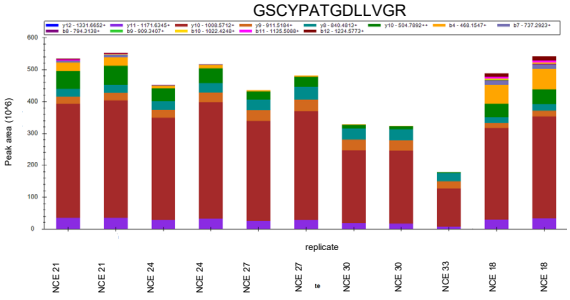

VLDPAIPIPDPYSSR

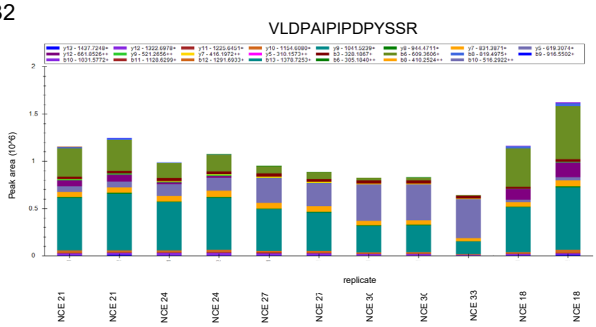

LYPA1

LAGVTALSCWLPLR

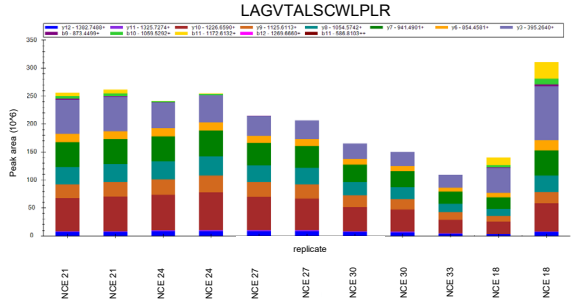

ASFPQGPIGGANR

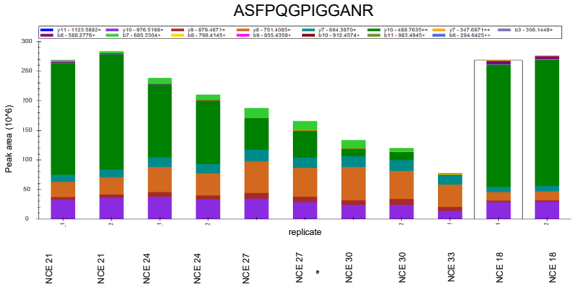

RHOB

IQAYDYLECSAK

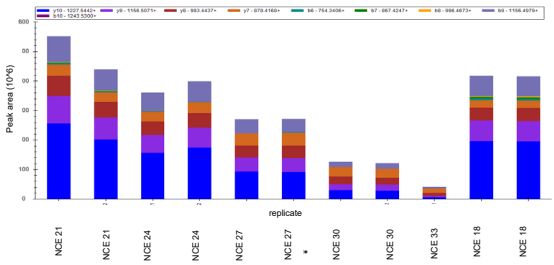

Supplemental Figure S15: Optimization of quadrupole mass isolation width for PRM analysis.

The optimization of the quadrupole isolation width, which determines the selectivity with which the peptide fragments proceed into further analysis, can enhance the performance of each PRM assay. Quadrupole mass isolation width was experimentally defined. Several values of quadrupole mass isolation width (0.5, 0.6, 0.7, 1, 1.4 m/z) were set using Q-Exactive™ Plus software and the signal produced by each peptide was monitored. Each bar graph shows the raw peak areas acquired for each peptide, with x-axis showing the applied quadrupole mass isolation width for each replicate. Each colour in each bar represents the signal contributed from individual transitions. Optimal isolation width corresponding to the greatest peak area for each peptide was selected. *PRM, Parallel reaction monitoring.*

S15

TSP1

GGVNDNFQGVLQNVR

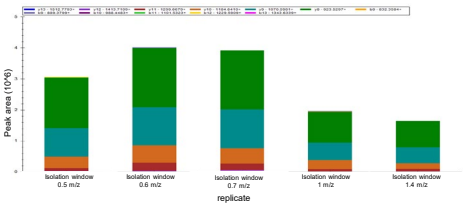

TIVTTLQDSIR

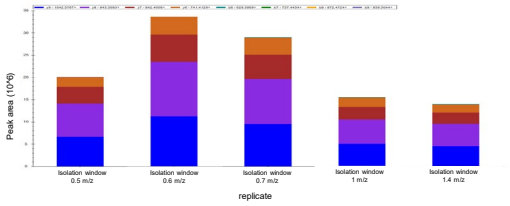

BST1

ALLSPEQR

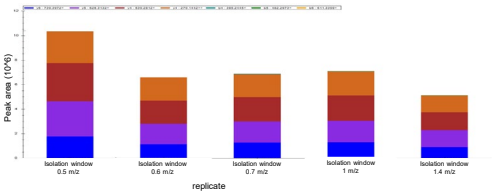

GFFADYEIPNLQK

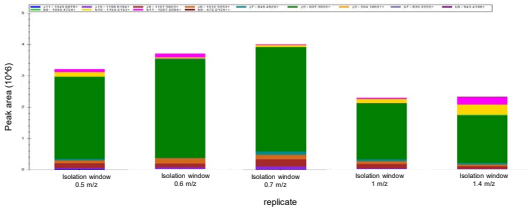

GLNA

LVLCEVFK

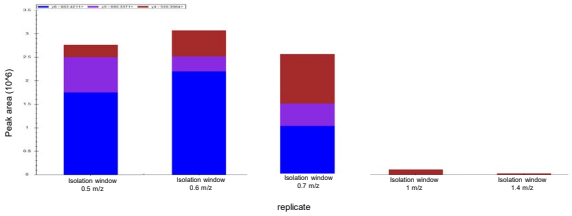

DIVEAHYR

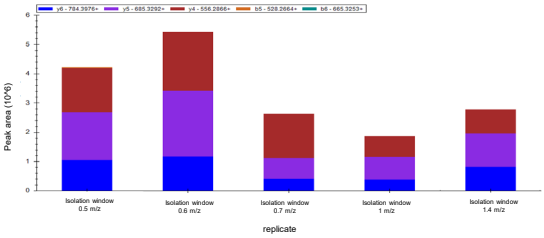

LAMB2

GSCYPATGDLLVGR

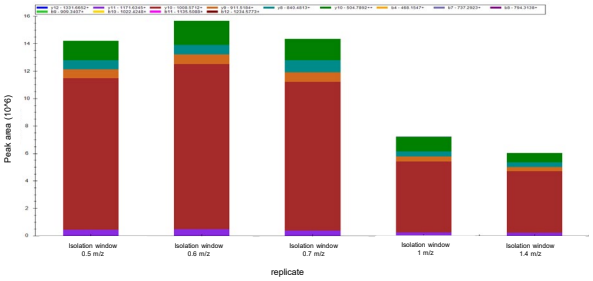

VLDPAIPIPDPYSSR

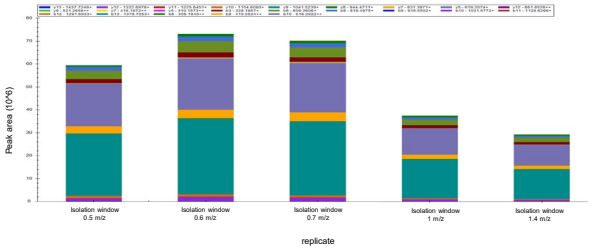

LYPA1

LAGVTALSCWLPLR

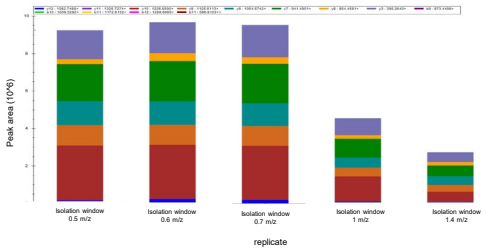

ASFPQGPIGGANR

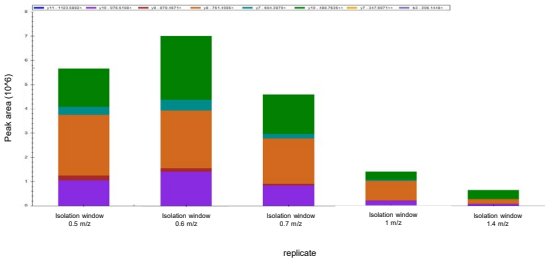

RHOB

IQAYDYLECSAK

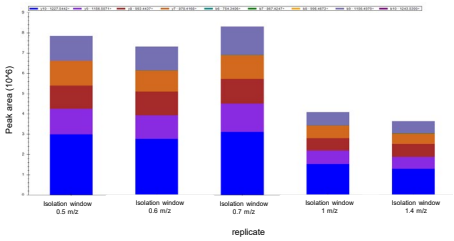

Supplemental Figure S16: Linearity curves for the peptides which have been selected for PRM analysis. Assay linearity was assessed for peptides ALLSPEQR and GFFADYEIPNLQK representing BST1, LVLCEVFK and DIVEAHYR representing GLNA, LAGVALSCWLPLR and ASFPQGPIGGANR representing LYPA1 and IQAYDYLECSAK representing RHOB protein. Linearity curves were prepared with different known amounts of heavy-labeled peptides and a constant concentration of endogenous peptides (BAL pool). The intensity area ratios of heavy-labeled peptides divided by the corresponding endogenous light peptides were plotted against the spiked heavy peptide concentrations. The samples representing each point of the linearity curve were run in duplicates. *PRM, parallel reaction monitoring; BST1, bone marrow stromal cell antigen 1; GLNA, glutamine synthetase; LYPA1, lysophospholipase 1; RHOB; ras homolog family member B.*

S16

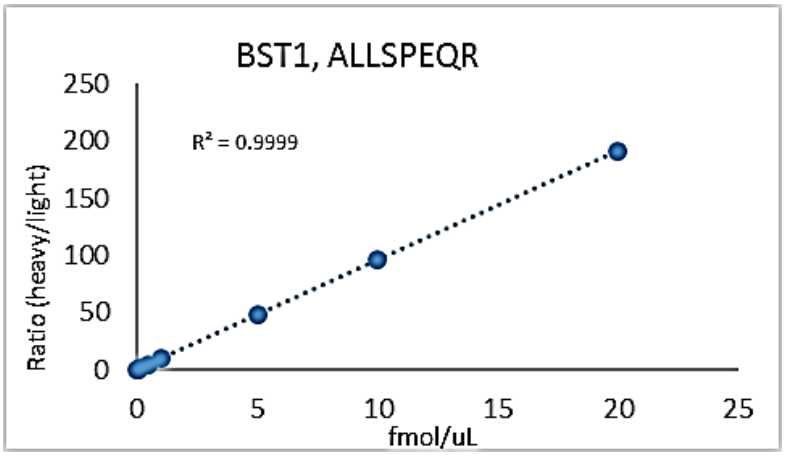
BST1, ALLSPEQR
R² = 0.9999
Ratio (heavy/light)
fmol/uL

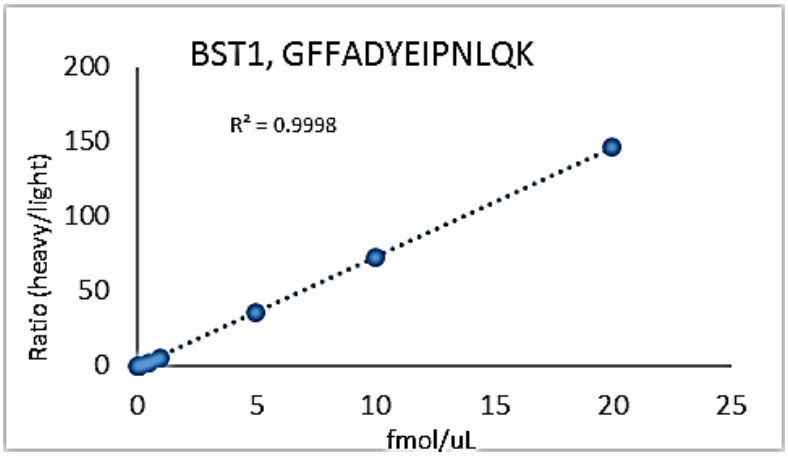
BST1, GFFADYEIPNLQK
R² = 0.9998
Ratio (heavy/light)
fmol/uL

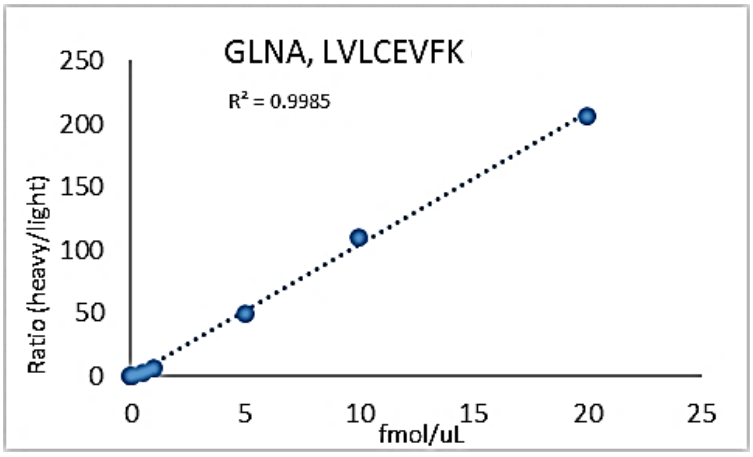
GLNA, LVLCEVFK
R² = 0.9985
Ratio (heavy/light)
fmol/uL

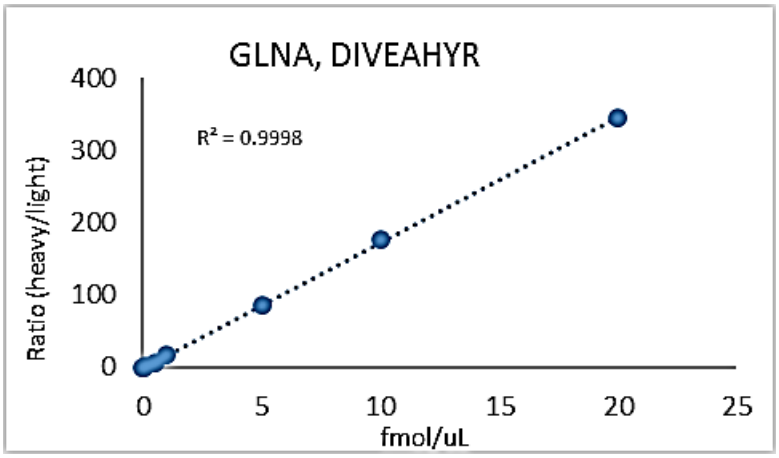
GLNA, DIVEAHYR
R² = 0.9998
Ratio (heavy/light)
fmol/uL

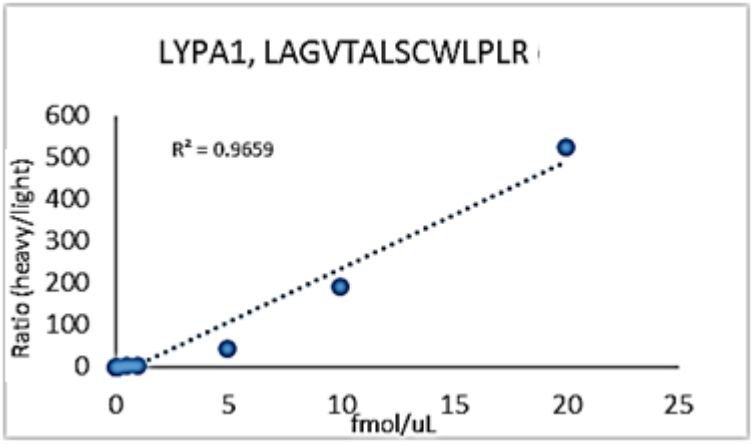
LYPA1, LAGVTALSCWLPLR
R² = 0.9659
Ratio (heavy/light)
fmol/uL

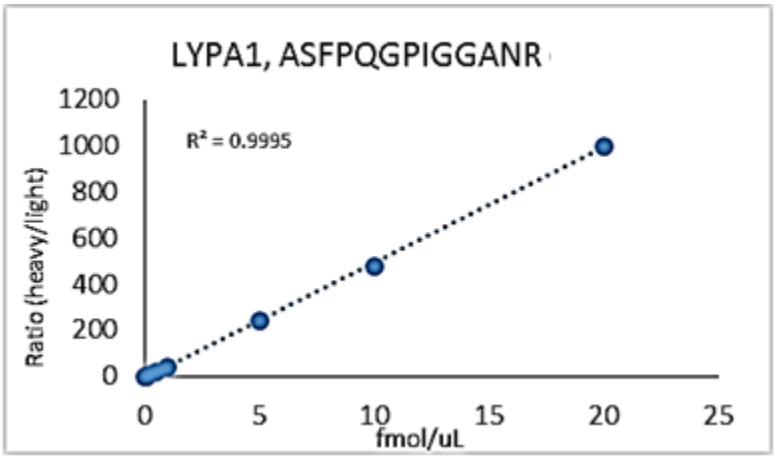
LYPA1, ASFPQGPIGGANR
R² = 0.9995
Ratio (heavy/light)
fmol/uL

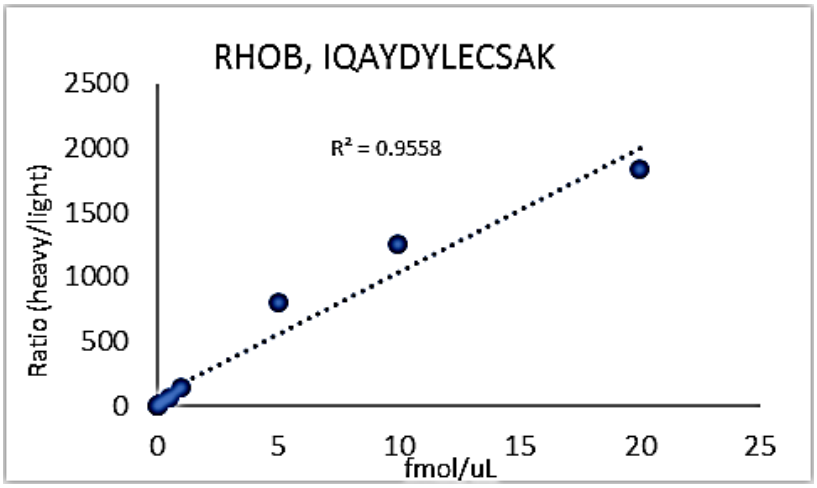
RHOB, IQAYDYLECSAK
R² = 0.9558
Ratio (heavy/light)
fmol/uL

Supplemental Table S1: Patient characteristics of lung tissue RT-qPCR cohort

	Controls (n=20)	BOS (n=18*)	RAS[o] (n=15*)	*p-value
Age at transplant, mean (SD)	NA	33 (19-42)	24.5 (19-36)	0.55
Age at CLAD onset, mean (SD)	NA	35.6 (14.2)	31.5 (12)	0.4
Age at sample collection, median (IQR)	62 (40-68)	38 (24-42)	28 (24-40)	**0.0019** [p]
Patient sex, male (%)	9 (45%)	5 (27.8%)	9 (60%)	0.17
Sex Match (D/R), n (%):				0.12
- M/F	NA	5 (27.8%)	3(20%)	
- M/M	NA	0 (0%)	5 (33.3%)	
- F/F	NA	7 (38.9%)	3 (20%)	
- F/M	NA	5 (27.8%)	3 (20%)	
- Donor information missing[t]	NA	1 (5.5%)	1 (6.7%)	
Smoking history, n (%)	9/20 (45%)[I]	7/18 (38.9%)[J]	7/15 (46.7%)[J]	0.88
Native lung disease, n (%):				0.26
- Pulmonary fibrosis	NA	6 (33.3%)	2 (13.3%)	
- Cystic fibrosis	NA	8 (44.4%)	11 (73.3%)	
- Chronic pulmonary obstructive disease	NA	1 (5.6%)	0 (0%)	
- Bronchiectasis	NA	3 (16.7%)	1 (6.7%)	
- Bronchopulmonary dysplasia	NA	0 (0%)	1 (6.7%)	
CMV Matching (R/D):				0.42
R-/D-	NA	2 (11.1%)	5 (33.3%)	
R+/D- and R+/D+	NA	10 (55.6%)	5 (33.3%)	
R-/D+	NA	5 (27.7%)	4 (26.7%)	
Donor information missing[t]		1 (5.6%)	1 (6.7%)	
Donor Type				0.92
- DBD	NA	12 (66.7%)	9 (60%)	
- DCD	NA	5 (27.8%)	5 (33.3%)	
- Unknown	NA	1 (5.5%)	1 (6.7%)	
Donor age, mean (SD)	NA	43.7 (15.8)	42.1 (15.9)	0.78
Donor lung processed by EVLP, n (%)	NA	5 (27.8%)	4 (26.7%)	0.94
Transplant related scores:				
- A score, median (IQR)	NA	0.27 (0-0.58)	0.31 (0.2-0.47)	0.72
- B score, median (IQR)	NA	0 (0-0)	0 (0-0.25)	0.96
- Infection score, mean (SD)	NA	0.38 (0.2)	0.35 (0.16)	0.64
Infectious status at the time of explant				0.95
- No infection, n (%)	NA	9 (50%)	7 (46.6%)	
- Colonization, n (%)	NA	5 (27.8%)	4 (26.7)	
- Active infection[x], n (%)	NA	4 (22.2%)	4 (26.7)	

[0] out of 15 RAS, 2 were actually mixed phenotype

[p] but the lung allograft age (based on the corresponding donor age) was comparable to the age of the control lungs

[I] 4/10 patients in the lobectomy subgroup and 5/10 in the donor lung subgroup.

[J] these numbers represent donors characteristics.

* clinical data are missing for one BOS and one RAS patients who weren't transplanted in our center.

[t] the patient was transplanted the first time in another center

[x] an active infection is defined by a positive culture and a specific antimicrobial treatment for less than 14 days at the time of explant.

CLAD, chronic lung allograft dysfunction; BOS, bronchiolitis obliterans syndrome; RAS, restrictive allograft syndrome; F, female; M, male; CMV, Cytomegalovirus; D, donor; R, recipient; DBD, donor after brain death; DCD, donation after circulatory death; EVLP, ex-vivo lung perfusion.

Distribution of demographic characteristics was tested by Kolmogorov-Smirnov test. The results are represented as mean and standard deviation (SD) for normally distributed variables, and as median and interquartile range (IQR) for non-normally distributed variables. *For comparison between three groups, we used one-way ANOVA or non-parametric equivalent.

Proportions of discrete variables were assessed by Chi-square and Fischer's exact test. If no data was available for the control group, comparison of mean/median of continuous variable in two groups was assessed by t-test/Mann-Whitney, respectively.

Supplemental Table S2: Patients characteristics of lung tissue immunostaining cohort

	Controls (n=5)	BOS (n=5)	RAS (n=5)	*p-value
Age at transplant, mean (SD)	NA	30 (16.4)	22 (3.74)	
Age at CLAD onset, mean (SD)	NA	34.4 (16.9)	24.6 (2.6)	
Age at collection of sample, mean (SD)	64.2 (19.02)	35.6 (17.7)	26.6 (1.82)	**0.005**[p]
Patient sex, male (%)	1 (20%)	0 (%)	4 (80%)	**0.02***
Sex matching (D/R):				0.06
- M/F	NA	3	0	
- M/M	NA	0	3	
- F/F	NA	2	1	
- F/M	NA	0	1	
Smoking history	3	3 [J]	2 [J]	0.77
Native lung disease :				0.44
- Pulmonary fibrosis	NA	2	0	
- Cystic fibrosis	NA	3	5	
CMV Matching (R/D):				0.13
R-/D-	NA	0	2	
R+/D- and R+/D+	NA	4	1	
R-/D+	NA	1	2	
Donor Type				0.89
- DBD	2	4	4	
- DCD	1	1	1	
Donor age, mean (SD)	NA	40.2 (8.9)	41 (10.1)	0.90
Donor lung processed by EVLP	NA	1	1	>0.99
Transplant related scores:				
- A score, mean (SD)	NA	0.34 (0.23)	0.31 (0.19)	0.86
- B score, mean (SD)	NA	0.13 (0.25)	0.27 (0.43)	0.58
- Infection score, mean (SD)	NA	0.27 (0.17)	0.3 (0.08)	0.39
Infectious status at the time of explant [x]				>0.99
- No infection, n (%)	NA	3	3	
- Colonization, n (%)	NA	2	2	

[p] but the lung allograft age (based on the corresponding donor age) was comparable to the age of the control lungs

[*] There is no statistical difference between controls and CLAD if BOS and RAS are analyzed together (Fisher's exact test p=0.6).

[J] these numbers represent donors characteristics.

[x] an active infection is defined by a positive culture and a specific antimicrobial treatment for less than 14 days at the time of explant.

CLAD, chronic lung allograft dysfunction; BOS, bronchiolitis obliterans syndrome; RAS, restrictive allograft syndrome; D, donor; R, recipient; DBD, donor after brain death; DCD, donation after circulatory death; CMV, Cytomegalovirus.

Distribution of demographic characteristics was tested by Kolmogorov-Smirnov test. The results are represented as mean and standard deviation (SD) for normally distributed variables, and as median and interquartile range (IQR) for non-normally distributed variables. *For comparison between three groups, we used one-way ANOVA or non-parametric equivalent.

Proportions of discrete variables were assessed by Chi-square and Fischer's exact test. If no data was available for the control group, comparison of mean/median of continuous variable in two groups was assessed by t-test/Mann-Whitney, respectively.

Supplemental Table S3: Primer list for RT-qPCR

Gene	Accession No.		Sequences (5' → 3')	Length (bp)	Amplicon size (bp)
hAGTR1	NM_000685	For	GCG CGG GTT TGA TAT TTG AC	20	135
		Rev	TGA TCA CCT GGG TCG AAT TTG	21	
hAGTR2	NM_000686	For	AGC AAG CTG ATT TAT GAT AAC TGC	24	145
		Rev	ACA AGC CCG AAG TGA AGA C	19	
hGLNA	NM_001033044	For	AGA GTC GAG AGT GGG AGA AG	20	148
		Rev	TGG GAA CTT GCT GAG GTG	18	
hTSP1	NM_003246	For	CTC CCC TAT GCT ATC ACA ACG	21	149
		Rev	AGG AAC TGT GGC ATT GGA G	19	
hLYPA1	NM_001279358.2	For	GCA ATA ACA TGT CAA CCC CG	20	134
		Rev	GTG AAC TTC TGA TAC CTG CAA AG	23	
hBST1	NM_004334.3	For	CTT GTC CAG GCA CTC TAT TCC	21	144
		Rev	CAG CTC AAG AAA TCT GCA ACC	21	

AGTR1, Angiotensin II-type 1 receptor ; AGTR2, Angiotensin II-type 2 receptor ; GLNA, glutamine synthetase ; TSP1, Thrombospondin 1; LYPA1, lysophospholipase 1 ; BST1, bone marrow stromal cell antigen 1 ; h, human ; No, number ; bp, base pair.

Supplemental Table S4: Inclusion list of PRM methods for monitoring AngII-regulated peptides

Protein	Peptide	Start (min)	End (min)	NCE
TSP1	GGVNDNFQGVLQNVR (light)	30.32	35.32	27
	GGVNDNFQGVLQNVR (heavy)	30.32	35.32	27
	TIVTTLQDSIR (light)	31.32	36.32	21
	TIVTTLQDSIR (heavy)	31.32	36.32	21
BST1	ALLSPEQR (light)	15.71	20.71	24
	ALLSPEQR (heavy)	15.71	20.71	24
	GFFADYEIPNLQK (light)	35.92	40.92	21
	GFFADYEIPNLQK (heavy)	35.92	40.92	21
GLNA	LVLCEVFK (light)	32.38	37.38	18
	LVLCEVFK (heavy)	32.38	37.38	18
	DIVEAHYR (light)	13.56	18.56	24
	DIVEAHYR (heavy)	13.56	18.56	24
LAMB2	GSCYPATGDLLVGR (light)	26.51	31.51	21
	GSCYPATGDLLVGR (heavy)	26.51	31.51	21
	VLDPAIPIPDPYSSR (light)	33.97	38.97	21
	VLDPAIPIPDPYSSR (heavy)	33.97	38.97	21
LYPA1	LAGVTALSCWLPLR (light)	46.04	51.04	21
	LAGVTALSCWLPLR (heavy)	46.04	51.04	21
	ASFPQGPIGGANR (light)	19.62	24.62	18
	ASFPQGPIGGANR (heavy)	19.62	24.62	18
RHOB	IQAYDYLECSAK (light)	25.17	30.17	21
	IQAYDYLECSAK (heavy)	25.17	30.17	21

RHOB, rho-related GTP-binding protein; BST1, bone marrow stromal cell antigen 1; GLNA, glutamine synthetase; LYPA1, lysophospholipase 1; TSP1, Thrombospondin 1 ; LAMB2, Laminin Subunit β2 ; NCE, Normalized collision energy.